Journal of Sound and Vibration 599 (2025) 118850

Contents lists available at ScienceDirect

Journal of Sound and Vibration

journal homepage: www.elsevier.com/locate/jsvi

Pole-zero placement through the robust receptance method for multi-input active vibration control with time delay

José Mário Araújo [a], Nelson J.B. Dantas [b], Carlos E.T. Dórea [b], Dario Richiedei [c], Iacopo Tamellin [d,*]

[a] Grupo de Pesquisa em Sinais e Sistemas, Instituto Federal de Educação, Ciência e Tencnologia da Bahia, Salvador 40301-015, Brazil
[b] Departamento de Engenharia de Computação e Automação, Universidade Federal do Rio Grande do Norte 59078-900 Natal, Brazil
[c] Department of Management and Engineering, University of Padova, Stradella S. Nicola 3, Vicenza 36100, Italy
[d] Department of Engineering for Innovation Medicine, University of Verona, Strada Le Grazie 15, Verona 37134, Italy

ARTICLE INFO

Keywords:
Active vibration control
Zero assignment
Partial pole placement
Time-delay
Receptance method
Robust control

ABSTRACT

Vibration control is fundamental to improve the performances of lightweight flexible systems. However, the introduction of sensors and actuators in the control loop introduces time-delays which must be carefully considered during the tuning stage to obtain effective controllers. This paper proposes a novel approach for the design of state and state-derivative feedback active vibration controllers in multi-input systems with time delay. The method exploits the versatility provided by the system receptances: two procedures are presented to compute the control gain matrices that simultaneously assign the antiresonance frequencies (zero assignment) and a subset of the desired closed-loop poles (partial pole placement). The notion of *eigenloci* of the loop gain, an extension of the Nyquist plot for multi-input systems, is used to impose closed-loop stability and guaranteed robustness margins to the closed-loop system. A Genetic Algorithm is exploited to search a solution of the control non-convex optimization problem. The effectiveness of the proposed method is assessed through numerical simulations on some benchmark systems taken from the literature. The obtained results highlight that besides assigning the prescribed zeros and poles, the proposed method enables to obtain stable closed-loop systems with guaranteed phase and gain margins.

1. Introduction

1.1. State of the art

The control of dynamic systems represented by second-order matrix differential equations, e.g. vibrating mechanical systems, has been the object of great research effort in the last decades. In particular, the so-called receptance method has attracted a lot of interest since this approach relies entirely on the system frequency domain model, which can be entirely obtained from experimental data, even with a reduced number of sensors and actuators [1], without requiring the time-consuming and error-prone updating of the analytical model.

* Corresponding author.
E-mail addresses: araujo@ieee.org (J.M. Araújo), nelson.dantas@dca.ufrn.br (N.J.B. Dantas), cetdorea@dca.ufrn.br (C.E.T. Dórea), dario.richiedei@unipd.it (D. Richiedei), iacopo.tamellin@univr.it (I. Tamellin).

https://doi.org/10.1016/j.jsv.2024.118850
Received 11 March 2024; Received in revised form 8 November 2024; Accepted 15 November 2024
Available online 22 November 2024
0022-460X/

One of the major applications of this control technique is vibration suppression [1,2]. Active vibration control involves the use of actuators and sensors. Thus, the presence of time delay in measurements or actuations is, in practice, unavoidable [3]. Depending on the amount of delay, a control design that does not take it into account can result in unexpected and poorer performances of the controlled system. Even worse, the stability of the system can be jeopardized. Directly handling the delay can be challenging from a mathematical point of view, since it introduces an irrational term into the receptance model of the system. Hence, its characteristic equation becomes transcendent, i.e. infinite-dimensional. It follows that the system features its dominant poles and an infinite number of secondary poles, referred to as latent roots.

The first design method for second order systems with time-delay using the receptance matrices relied on the placement of a given number of poles for single input systems [4]. The problem of partial pole placement, i.e., assigning some poles by keeping unchanged the remaining with respect to the open-loop configuration, with single input control has been lately solved in [5]. The extension of the receptance method to more control actuators (the so-called multi-input control) has been lately proposed in [2] for systems without time delay. Then, partial pole placement with time delay has been solved in [6]. A method for high-order systems with time delay has been proposed in [7] and [8]. All these methods despite ensuring the desired placement of the dominant roots of the system do not guarantee closed-loop stability. Indeed, the transcendental nature of the problem yields the abovementioned latent roots whose placement in the complex plane, and then their stability had to be checked *a posteriori*. Stability can be evaluated through the simulation of the closed-loop system response or by evaluating the placement of both the dominant and latent roots through ad-hoc developed toolboxes (e.g. [9]). Alternatively, it is possible to exploit the many stability assessment criteria that have been proposed in the literature formulated with [10,11] and without the system receptances [12,13].

Such a problem has been recently tackled in [14] using the Linear Matrix Inequalities and the stability has been imposed *a priori*. However, this method requires the knowledge of the system matrices. In case only the receptance model is available, frequency response analysis methods emanating from the classical control theory can be employed [15]. In particular, the so-called Nyquist criterion allows to establish if a time-delay system is closed-loop stable with no need to resort to either approximations of the delay term or *a posteriori* checks. This idea has been used in [16] to propose an optimization-based control design of single-input second order time-delay systems with a given robustness margin. This robust receptance method has been further extended in [17] to include partial pole placement and applied to a flexible two-link flexible robotic arm in [18].

1.2. Contributions of the paper

The literature review highlights that pole assignment in systems with time delay has been extensively studied both in the single-input and in the multi-input scenario. Conversely, the assignment of zeros through receptance-based methods has been rarely investigated to the best of the authors knowledge. Zeros are fundamental for vibrating system, indeed when they appear in complex conjugate pairs, they yield an antiresonance which is a frequency at which the system experiences no vibrations for some excitation and response pairs. This feature of antiresonances is particularly attractive for vibration suppression, confinement and absorption.

In this light, this paper extends the methods proposed by the authors in [16] and [19] with two goals. First, the zero-assignment problem in multi-input systems, that has been up to now solved for pure second-order systems, is here extended to handle the presence of time-delay. Then, it is extended to the pole-zero assignment problem with time-delay.

Then, a robustness requirement is formulated in terms of the system receptances and is embedded in the problem to impose *a priori* the robust stability of the closed-loop system. This aspect is solved exploiting the so-called *eigenloci* plot [20] which enables to handle multiple frequency responses associated with the inputs.

The novel method proposed in this manuscript can be divided into two stages:

- An assignment stage in which receptance-based multi-input pole-zero assignment with time delay is solved;
- An optimization stage in which closed-loop stability and robustness of the controlled system is achieved without altering the placement of the poles and zeros assigned in the previous stage.

Two different methods are proposed in the assignment stage: a single-step and a multiple-step method. While, in the optimization stage, the problem of computing the controller gains that guarantee the prescribed robust stability margin defined over the eigenloci is solved through an ad-hoc developed Genetic Algorithm (GA).

The methods here proposed handles multiple time delays in both the measurements and the actuation. Further, both the design of state and state-derivative feedback controllers can be performed. Lastly, the method is formulated in terms of the system receptances, however it can be applied also in case only the system model is known, and experimental data are not available.

The effectiveness of the proposed methods is illustrated through several numerical simulations taken from the literature.

2. Theoretical background and problem statement

2.1. System model and definitions

The model of a linear second-order N-DOF vibrating system is written in the Laplace s-domain:

$$\left(s^2\mathbf{M} + s\mathbf{C} + \mathbf{K}\right)\mathbf{x}(s) = \mathbf{f_e}(s) \tag{1}$$

$\mathbf{M} \in \mathbb{R}^{N\times N}$, $\mathbf{C} \in \mathbb{R}^{N\times N}$, and $\mathbf{K} \in \mathbb{R}^{N\times N}$ are the system mass, damping and stiffness matrices, respectively; $\mathbf{x}(s) \in \mathbb{C}^N$ is the Laplace transform of the displacement vector $\underline{\mathbf{x}}(t) \in \mathbb{R}^N$ (all along the paper, the bars denote the variables in the time domain); $\mathbf{f_e}(s) \in \mathbb{C}^N$ is the vector of the external forces. By introducing the receptance matrix of the open-loop system $\mathbf{H}(s) = (s^2\mathbf{M} + s\mathbf{C} + \mathbf{K})^{-1}$, Eq. (1) becomes:

$$\mathbf{x}(s) = \mathbf{H}(s)\mathbf{f_e}(s) \tag{2}$$

Receptance $h_{pq}(s)$ is the pq-th entry of $\mathbf{H}(s)$ and it is the transfer function from the force applied to the q-th coordinate to the displacement of the p-th coordinate. In accordance with the Cramer's rule [21,22] it can be computed as:

$$h_{pq}(s) = \frac{x_p(s)}{f_q(s)} = (-1)^{p+q}\frac{\det\left(s^2\mathbf{M}_{\overline{qp}} + s\mathbf{C}_{\overline{qp}} + \mathbf{K}_{\overline{qp}}\right)}{\det(s^2\mathbf{M} + s\mathbf{C} + \mathbf{K})} \tag{3}$$

Removing the q-th row and the p-th column from matrices **M, C, K** yields the adjunct system matrices $\mathbf{M}_{\overline{qp}}, \mathbf{C}_{\overline{qp}}, \mathbf{K}_{\overline{qp}} \in \mathbb{R}^{(N-1)\times(N-1)}$. By following the notation proposed in [23] and recently exploited in [19], the following relations hold:

$$\mathbf{M}_{\overline{qp}} = \mathbf{B_n}^T\mathbf{M}\mathbf{C_n}, \quad \mathbf{C}_{\overline{qp}} = \mathbf{B_n}^T\mathbf{C}\mathbf{C_n}, \quad \mathbf{K}_{\overline{qp}} = \mathbf{B_n}^T\mathbf{K}\mathbf{C_n} \tag{4}$$

matrices $\mathbf{B_n}$ and $\mathbf{C_n}$ are obtained through the null space operator of vector $\boldsymbol{e}_q$ (column vector whose entries are all equal to zero except for the q-th entry which is equal to one) and $\boldsymbol{e}_p$ (column vector whose entries are all equal to zero except for the p-th entry which is equal to one):

$$\mathbf{B_n} = \text{null}\left(\mathbf{e}_q^T\right), \quad \mathbf{C_n} = \text{null}\left(\mathbf{e}_p\right) \tag{5}$$

It should be noted that receptances can be either numerically obtained from the system matrices as shown in Eq. (3) (e.g., when designing control for new systems through analytical models) or experimentally determined through measurements on existing systems ([1,24–26]).

The poles p_i, $i = 1, \ldots, 2N$ of the open-loop (uncontrolled) system can be obtained from the denominator of Eq. (3) or solving the following eigenproblem [19]:

$$\left(p_i^2\mathbf{M} + p_i\mathbf{C} + \mathbf{K}\right)\mathbf{u}_{p,i} = \mathbf{0}, \quad i = 1, \ldots, 2N \tag{6}$$

where $\mathbf{u}_{p,i} \in \mathbb{C}^N$ is the i th eigenvector related to the i th complex pole p_i.

The zeros z_i, $1 \le i \le 2(N-1)$ of receptance h_{pq} are obtained from the numerator of Eq. (3) or alternatively from the solution of the adjunct system eigenproblem [19]:

$$\left(z_i^2\mathbf{M}_{\overline{qp}} + z_i\mathbf{C}_{\overline{qp}} + \mathbf{K}_{\overline{qp}}\right)\mathbf{u}_{z,i} = \mathbf{0}, \quad 1 \le i \le 2(N-1) \tag{7}$$

where the i th complex zero is z_i and $\mathbf{u}_{z,i} \in \mathbb{C}^{N-1}$ is the i th right-eigenvector of the adjunct system, whose physical meaning has been discussed in [19,23].

For control design purpose, thanks to the system linearity, the disturbance forces can be discarded by just including the control forces $\mathbf{u}(s) \in \mathbb{C}^m$ (m is the number of independent actuators) among $\mathbf{f_e}(s)$ leading to $\mathbf{f_e}(s) = \mathbf{B}\mathbf{u}(s)$, where $\mathbf{B} \in \mathbb{R}^{N\times m}$ is the control force distribution matrix. By assuming state feedback control, in the presence of delayed speed and position measurements (with τ_F and τ_G being the delays on speed and displacement measurements, respectively) control forces in the time domain, $\underline{\mathbf{u}}(t) \in \mathbb{R}^m$, are computed as follows:

$$\underline{\mathbf{u}}(t) = \mathbf{F}^T\dot{\underline{\mathbf{x}}}(t-\tau_F) + \mathbf{G}^T\underline{\mathbf{x}}(t-\tau_G) \tag{8}$$

leading to the following dynamic model of the closed-loop system in the Laplace domain:

$$\left(s^2\mathbf{M} + s\mathbf{C} + \mathbf{K}\right)\mathbf{x}(s) = \mathbf{B}\left(s\mathbf{F}^T e^{-s\tau_F} + \mathbf{G}^T e^{-s\tau_G}\right)\mathbf{x}(s) \tag{9}$$

Alternatively, if state-derivative feedback is assumed (and let τ_D be the time delay affecting acceleration measurements) the following definition of $\underline{\mathbf{u}}(t)$ holds:

$$\underline{\mathbf{u}}(t) = \mathbf{D}^T\ddot{\underline{\mathbf{x}}}(t-\tau_D) + \mathbf{F}^T\dot{\underline{\mathbf{x}}}(t-\tau_F) \tag{10}$$

$\mathbf{D}, \mathbf{F}, \mathbf{G} \in \mathbb{R}^{N\times m}$ are the gain matrices, whose computation is discussed in this paper.

In Eqs. (8) and (10) no reference is assumed and a regulation problem is formulated: on one hand the reference does not affect the eigenstructure; on the other one, setting a zero reference is typical in vibration absorption problems.

It should be, finally, noticed that the proposed approach holds in the case of delay on the actuation forces as well, with obvious modifications.

Time-delayed systems, as the one in Eq. (9), features an infinite number of roots in their transcendental characteristic equation, which can be grouped into primary and secondary (or latent) roots [14]. In particular, their stability should be imposed *a priori* by exploiting some degrees of freedom in the controller design.

2.2. Control objectives and paper overview

The following control problems are addressed in this paper:

- Compute the state feedback gain matrices $\mathbf{F}$ and $\mathbf{G}$ such that the prescribed $n_p < N$ closed-loop poles and/or n_z zeros are assigned for the receptance $\overline{h}_{pq}$, and simultaneously impose stability and the required robustness of the closed-loop system;
- Compute the state-derivative feedback gain matrices $\mathbf{D}$ and $\mathbf{F}$ such that the prescribed $n_p < N$ closed-loop poles and/or n_z zeros are assigned of the receptance $\overline{h}_{pq}$, and simultaneously ensure the stability and the required robustness for the closed-loop system.

Two techniques, that handle both the state and the state-derivative feedback scenarios, are proposed to cope with the pole-zero assignment task, by extending two methods proposed by some of the authors of this paper in [19] for systems without time delay.

- The "single-step" method (Sections 3.1.1, 3.2.1, 3.3.1 and 3.4.1), that assigns the prescribed poles and zeros through the solution of a linear system;
- The "multi-step" method (Sections 3.1.2, 3.2.2, 3.3.2 and 3.4.2), that assigns the prescribed poles and zeros through the solution of m linear systems.

Then, in Section 4 a strategy that relies on the Generalized Nyquist contour (*eigenloci*) is explained to impose stability and to achieve the required robustness. This problem is solved through a genetic algorithm.

3. Multi-input control by the receptance method

3.1. Zero placement by the receptance method: state feedback

3.1.1. The single-step approach for the zero assignment

The zeros of the closed-loop receptance $\overline{h}_{pq}$ can be obtained solving the adjunct system eigenproblem in the controlled system. For convenience let us exploit the formalism of Eq. (4) to recast Eq. (9), and to obtain the eigenproblem of the closed-loop adjunct system:

$$\mathbf{B}_{\mathbf{n}}^T\left(\overline{z}_i^2\mathbf{M}+\overline{z}_i\mathbf{C}+\mathbf{K}\right)\mathbf{C}_{\mathbf{n}}\mathbf{w}_i = \mathbf{B}_{\mathbf{n}}^T\mathbf{B}\left(\overline{z}_i\mathbf{F}^T\mathrm{e}^{-\overline{z}_i\tau_F}+\mathbf{G}^T\mathrm{e}^{-\overline{z}_i\tau_G}\right)\mathbf{C}_{\mathbf{n}}\mathbf{w}_i, \quad i=1,\dots,n_z \tag{11}$$

where $\mathbf{w}_i \in \mathbb{C}^{N-1}$ is the i th adjunct system right eigenvector related to the zero $\overline{z}_i$ to assign.

Let us define the receptance matrix of the adjunct system, evaluated for $s = \overline{z}_i$, as follows:

$$\mathbf{H}_{\overline{qp}}(\overline{z}_i) = \left(\mathbf{B}_{\mathbf{n}}^T\left(\overline{z}_i^2\mathbf{M}+\overline{z}_i\mathbf{C}+\mathbf{K}\right)\mathbf{C}_{\mathbf{n}}\right)^{-1} \tag{12}$$

where $\mathbf{H}_{\overline{qp}}(\overline{z}_i)$ can be computed from the system matrices as follows [19,21]:

$$\mathbf{H}_{\overline{qp}}(\overline{z}_i) = \left(\overline{z}_i^2\mathbf{M}_{\overline{qp}}+\overline{z}_i\mathbf{C}_{\overline{qp}}+\mathbf{K}_{\overline{qp}}\right)^{-1} \tag{13}$$

$\mathbf{H}_{\overline{qp}}(\overline{z}_i)$ can be simply determined numerically from the measured receptances of the original system $\mathbf{H}(\overline{z}_i)$, without involving the system matrices, through the following relations:

$$\mathbf{H}(\overline{z}_i)\rightarrow\mathbf{Z}(\overline{z}_i) = \mathbf{H}^{-1}(\overline{z}_i)\rightarrow\mathbf{Z}_{\overline{qp}}(\overline{z}_i) = \mathbf{B}_{\mathbf{n}}^T\mathbf{Z}(\overline{z}_i)\mathbf{C}_{\mathbf{n}}\rightarrow\mathbf{H}_{\overline{qp}}(\overline{z}_i) = \mathbf{Z}_{\overline{qp}}^{-1}(\overline{z}_i) \tag{14}$$

By exploiting Eq. (12), Eq. (11) is recast in terms of the adjunct system measured receptances:

$$\mathbf{w_i} = \mathbf{H}_{\overline{qp}}(\overline{z}_i)\widetilde{\mathbf{B}}\left(\overline{z}_i\widetilde{\mathbf{F}}^T\mathrm{e}^{-\overline{z}_i\tau_F}+\widetilde{\mathbf{G}}^T\mathrm{e}^{-\overline{z}_i\tau_G}\right)\mathbf{w_i}, \quad i=1,\dots,n_z \tag{15}$$

where:

$$\begin{aligned}\widetilde{\mathbf{B}} &= \mathbf{B}_{\mathbf{n}}^T\mathbf{B} \in \mathbb{R}^{(N-1)\times m}\\ \widetilde{\mathbf{F}}^T &= \mathbf{F}^T\mathbf{C}_{\mathbf{n}} \in \mathbb{R}^{m\times(N-1)}\\ \widetilde{\mathbf{G}}^T &= \mathbf{G}^T\mathbf{C}_{\mathbf{n}} \in \mathbb{R}^{m\times(N-1)}\end{aligned} \tag{16}$$

The matrices in Eq. (16) can be partitioned as: $\widetilde{\mathbf{B}} = [\widetilde{\mathbf{b}}_1 \quad \dots \quad \widetilde{\mathbf{b}}_m]$, $\widetilde{\mathbf{F}} = [\widetilde{\mathbf{f}}_1 \quad \dots \quad \widetilde{\mathbf{f}}_m]$ and $\widetilde{\mathbf{G}} = [\widetilde{\mathbf{g}}_1 \quad \dots \quad \widetilde{\mathbf{g}}_m]$. Hence, Eq. (15) is equivalent to:

$$\mathbf{w}_i = \mathbf{H}_{\overline{qp}}(\overline{z}_i)\left(\widetilde{\mathbf{b}}_1\left(\overline{z}_i\widetilde{\mathbf{f}}_1^T\mathrm{e}^{-\overline{z}_i\tau_F}+\widetilde{\mathbf{g}}_1^T\mathrm{e}^{-\overline{z}_i\tau_G}\right)+\dots+\widetilde{\mathbf{b}}_m\left(\overline{z}_i\widetilde{\mathbf{f}}_m^T\mathrm{e}^{-\overline{z}_i\tau_F}+\widetilde{\mathbf{g}}_m^T\mathrm{e}^{-\overline{z}_i\tau_G}\right)\right), \quad i=1,\dots,n_z \tag{17}$$

Eq. (17) can be transformed in the following convenient form:

$$\mathbf{w}_i = \alpha_{i,1}\boldsymbol{\psi}_{i,1}+\dots+\alpha_{i,m}\boldsymbol{\psi}_{i,m}, \quad j=1,\dots,m \tag{18}$$

by defining

$$\boldsymbol{\psi}_{i,j} = \mathbf{H}_{\overline{q}\overline{p}}(\overline{z}_i)\widetilde{\mathbf{b}}_j, \quad i = 1, \ldots, n_z \text{ and } j = 1, \ldots, m \tag{19}$$

and by considering that, as discussed in [2] for partial pole placement, some scalar coefficients $\alpha_{i,j}$ can be arbitrary chosen in such a way that:

$$\alpha_{i,j} = \left(\overline{z}_i \widetilde{\mathbf{f}}_m^T \mathrm{e}^{-s\tau_F} + \widetilde{\mathbf{g}}_m^T \mathrm{e}^{-s\tau_G}\right)\mathbf{w}_i, \quad i = 1, \ldots, n_z \text{ and } j = 1, \ldots, m \tag{20}$$

Eq. (18) reveals that the attainable right-eigenvectors of the adjunct system are a linear combination of vectors $\boldsymbol{\psi}_{i,j}$, which in turn depends on the system parameters by means of $\mathbf{H}_{\overline{q}\overline{p}}(\overline{z}_i)$ and on the actuation matrix $\mathbf{B}$ partitioned through $\widetilde{\mathbf{b}}_j$, $j = 1, \ldots, m$. Besides that, the right-eigenvectors of the adjunct system depends on the chosen modal vector coefficients $\alpha_{i,j}$ which is arbitrary and up to the designer of the control system.

Eq. (20) can be transposed and recast in the form of a linear system

$$\begin{bmatrix} \overline{z}_i \mathbf{w}_i^T \mathrm{e}^{-\overline{z}_i\tau_F} & \mathbf{0} & \cdots & \mathbf{0} & \mathbf{w}_i^T \mathrm{e}^{-\overline{z}_i\tau_G} & \mathbf{0} & \cdots & \mathbf{0} \\ \mathbf{0} & \overline{z}_i \mathbf{w}_i^T \mathrm{e}^{-\overline{z}_i\tau_F} & \cdots & \mathbf{0} & \mathbf{0} & \mathbf{w}_i^T \mathrm{e}^{-\overline{z}_i\tau_G} & \cdots & \mathbf{0} \\ \vdots & \vdots & \ddots & \vdots & \vdots & \vdots & \ddots & \vdots \\ \mathbf{0} & \mathbf{0} & \cdots & \overline{z}_i \mathbf{w}_i^T \mathrm{e}^{-\overline{z}_i\tau_F} & \mathbf{0} & \mathbf{0} & \cdots & \mathbf{w}_i^T \mathrm{e}^{-\overline{z}_i\tau_G} \end{bmatrix} \begin{Bmatrix} \widetilde{\mathbf{f}}_1 \\ \vdots \\ \widetilde{\mathbf{f}}_m \\ \widetilde{\mathbf{g}}_1 \\ \vdots \\ \widetilde{\mathbf{g}}_m \end{Bmatrix} = \begin{Bmatrix} \alpha_{i,1} \\ \vdots \\ \alpha_{i,m} \end{Bmatrix} \tag{21}$$

Eq. (21) can be summarized in the following form, with the obvious meaning of symbols, that represents the assignment of the i th zero $\overline{z}_i$:

$$\boldsymbol{\Phi}_{\mathbf{sz},i}\widetilde{\mathbf{k}}_{\mathbf{s}} = \boldsymbol{\alpha}_{\mathbf{z},i} \tag{22}$$

By collecting all the assignment equations of the prescribed n_z zeros:

$$\begin{bmatrix} \boldsymbol{\Phi}_{\mathbf{sz},1} \\ \vdots \\ \boldsymbol{\Phi}_{\mathbf{sz},n_z} \end{bmatrix} \widetilde{\mathbf{k}}_{\mathbf{s}} = \begin{Bmatrix} \boldsymbol{\alpha}_{\mathbf{z},1} \\ \vdots \\ \boldsymbol{\alpha}_{\mathbf{z},n_z} \end{Bmatrix} \tag{23}$$

Eq. (23) in turn can be recast in the more compact form:

$$\boldsymbol{\Phi}_{\mathbf{sz}}\widetilde{\mathbf{k}}_{\mathbf{s}} = \boldsymbol{\alpha}_{\mathbf{z}} \tag{24}$$

The state feedback control gains are obtained by solving the linear system in Eq. (24). If the set of the desired zeros is self-conjugated (and the system is controllable), matrices $\widetilde{\mathbf{F}}$ and $\widetilde{\mathbf{G}}$ are real [2,19].

After solving Eq. (24), $\widetilde{\mathbf{F}}$ and $\widetilde{\mathbf{G}}$ should be transformed into the gain matrices $\mathbf{F}$ and $\mathbf{G}$ by considering that the columns of $\mathbf{C}_\mathbf{n}$ are orthonormal, and hence $\mathbf{C}_\mathbf{n}^T\mathbf{C}_\mathbf{n} = \mathbf{I}_{N-1}$. Inversion of Eq. (16) leads therefore to:

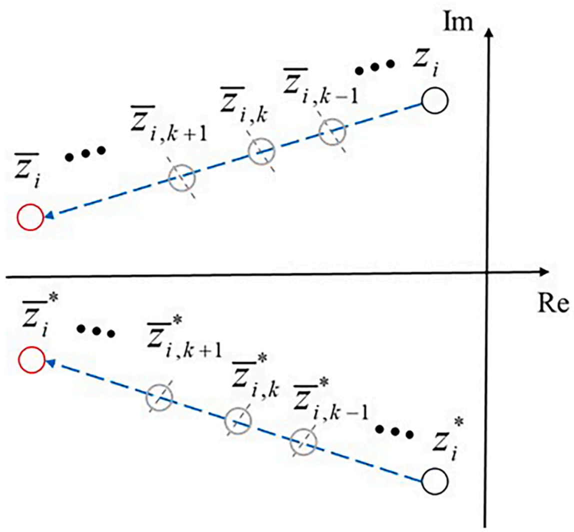

Fig. 1. Multi-step assignment from the i th open-loop zero (black) to the i th prescribed zero (red).

$$\mathbf{F}^T = \widetilde{\mathbf{F}}^T\mathbf{C}_\mathbf{n}^T$$
$$\mathbf{G}^T = \widetilde{\mathbf{G}}^T\mathbf{C}_\mathbf{n}^T \tag{25}$$

3.1.2. The multi-step approach for the zero assignment

The chief idea of the multi-step approach is to treat the m-rank assignment as a sequence of m rank-one assignments. To cope with this task, a placement path from the original system zeros to the desired ones through m assignment steps (i.e. the same number of the actuators) must be defined. Fig. 1 shows an example of assignment path in the case of a pair of complex conjugate zeros.

The actuation matrix and the control gain matrices are partitioned into: $\mathbf{B} = [\mathbf{b}_1 \quad \dots \quad \mathbf{b}_m]$, $\mathbf{F} = [\mathbf{f}_1 \quad \dots \quad \mathbf{f}_m]$ and $\mathbf{G} = [\mathbf{g}_1 \quad \dots \quad \mathbf{g}_m]$. For each step of the proposed method (denoted by index $k = 1,\dots, m$) the set of the prescribed zeros is assigned at the k-th step $\{\overline{z}_{1,k}, \dots, \overline{z}_{n_z,k}\}$ by means of the control gains $\boldsymbol{f}_k, \boldsymbol{g}_k$. Hence, after the m-steps the prescribed zeros $\{\overline{z}_1, \dots, \overline{z}_{n_z}\}$ are assigned and the gain matrices $\mathbf{F}$ and $\mathbf{G}$ are completely determined.

The control gains that enable to assign the set of the prescribed zeros at the generic k-th step are computed by adapting the single-input ($m = 1$) receptance method proposed in [4,17] to the scenario of zero assignment with time delay. In the single-input case, the receptance matrix of the closed-loop system $\overline{\mathbf{H}}(s)$ at the k-th step is defined as:

$$\overline{\mathbf{H}}_k(s) = \left(s^2\mathbf{M} + s\left(\mathbf{C}_{k-1} - \mathbf{b}_k\mathbf{f}_k^T\mathrm{e}^{-s\tau_F}\right) + \left(\mathbf{K}_{k-1} - \mathbf{b}_k\mathbf{g}_k^T\mathrm{e}^{-s\tau_G}\right)\right)^{-1} \tag{26}$$

where: $\mathbf{C}_{k-1} = \mathbf{C} - [\mathbf{b}_1 \quad \dots \quad \mathbf{b}_{k-1}][\mathbf{f}_1\mathrm{e}^{-s\tau_F} \quad \dots \quad \mathbf{f}_{k-1}\mathrm{e}^{-s\tau_F}]^T$ and $\mathbf{K}_{k-1} = \mathbf{K} - [\mathbf{b}_1 \quad \dots \quad \mathbf{b}_{k-1}][\mathbf{g}_1\mathrm{e}^{-s\tau_G} \quad \dots \quad \mathbf{g}_{k-1}\mathrm{e}^{-s\tau_G}]^T$.

The Sherman-Morrison formula together with some algebraic manipulations leads to the receptance $\overline{h}_{pq,k}$ at the k-th step as:

$$\overline{h}_{pq,k}(s) = \frac{\mathbf{e}_p^T\left[\left(1 - (s\mathbf{f}_k e^{-s\tau_F} + \mathbf{g}_k\mathrm{e}^{-s\tau_G})^T\overline{\mathbf{H}}_{k-1}(s)\mathbf{b}_k\right)\overline{\mathbf{H}}_{k-1}(s) + \overline{\mathbf{H}}_{k-1}(s)\mathbf{b}_k(s\mathbf{f}_k\mathrm{e}^{-s\tau_F} + \mathbf{g}_k\mathrm{e}^{-s\tau_G})^T\overline{\mathbf{H}}_{k-1}(s)\right]\mathbf{e}_q}{1 - (s\mathbf{f}_k\mathrm{e}^{-s\tau_F} + \mathbf{g}_k\mathrm{e}^{-s\tau_G})^T\overline{\mathbf{H}}_{k-1}(s)\mathbf{b}_\mathbf{k}} \tag{27}$$

The zeros of the system at the k-th step are the roots of the numerator of Eq. (27). Let us define the auxiliary complex vector $\mathbf{t}_{i,k} = h_{rc,k-1}(\overline{z}_{i,k})\overline{\mathbf{H}}_{k-1}(\overline{z}_{i,k})\mathbf{b}_k - \left[\mathbf{e}_p^T\overline{\mathbf{H}}_{k-1}(\overline{z}_{i,k})\mathbf{b}_k\right]\overline{\mathbf{H}}_{k-1}(\overline{z}_{i,k})\mathbf{e}_q$ evaluated at the i th prescribed zero $\overline{z}_{i,k}$. The n_z assignment problems at the k-th step are collected in the linear system:

$$\begin{bmatrix} \overline{z}_{1,k}\mathbf{t}_{1,k}^T\mathrm{e}^{-\overline{z}_{1,k}\tau_F} & \mathbf{t}_{1,k}^T\mathrm{e}^{-\overline{z}_{1,k}\tau_G} \\ \overline{z}_{2,k}\mathbf{t}_{2,k}^T\mathrm{e}^{-\overline{z}_{2,k}\tau_F} & \mathbf{t}_{2,k}^T\mathrm{e}^{-\overline{z}_{2,k}\tau_G} \\ \vdots & \vdots \\ \overline{z}_{n_z,k}\mathbf{t}_{n_z,k}^T\mathrm{e}^{-\overline{z}_{n_z,k}\tau_F} & \mathbf{t}_{n_z,k}^T\mathrm{e}^{-\overline{z}_{n_z,k}\tau_G} \end{bmatrix} \begin{Bmatrix} \mathbf{f}_k \\ \mathbf{g}_k \end{Bmatrix} = \begin{Bmatrix} h_{pq,k-1}(\overline{z}_{1,k}) \\ h_{pq,k-1}(\overline{z}_{2,k}) \\ \vdots \\ h_{pq,k-1}(\overline{z}_{n_z,k}) \end{Bmatrix} \tag{28}$$

The demonstration of Eq. (28) is provided in Appendix A.

In a more compact form, the linear system is recast into:

$$\boldsymbol{\Phi}_{\mathbf{sz},k}\mathbf{k}_{\mathbf{s},k} = \mathbf{y}_{\mathbf{z},k} \tag{29}$$

The solution of Eq. (28) for $k = 1, \dots, m$ yields the gain matrices $\mathbf{F}$ and $\mathbf{G}$.

3.2. Zero assignment through state-derivative feedback

3.2.1. The single-step approach for the zero assignment in the state-derivative case

The zero assignment problem through the single-step method in the case of state-derivative feedback (see Eq. (10)) is obtained by reformulating Eq. (15) as follows:

$$\mathbf{w}_i = \mathbf{H}_{\overline{qp}}(\overline{z}_i)\widetilde{\mathbf{B}}\left(\overline{z}_i^2\widetilde{\mathbf{D}}^T\mathrm{e}^{-\overline{z}_i\tau_D} + \overline{z}_i\widetilde{\mathbf{F}}^T\mathrm{e}^{-\overline{z}_i\tau_F}\right)\mathbf{w}_i, \quad i = 1, \dots, n_z \tag{30}$$

with $\widetilde{\mathbf{D}}^T = \mathbf{D}^T\mathbf{C}_\mathbf{n} \in \mathbb{R}^{m\times(N-1)}$ the acceleration gains matrix in the adjunct system. The linear system for the assignment of the i th zero is obtained through similar steps as those introduced in Section 3.1.1:

$$\begin{bmatrix} \overline{z}_i^2\mathbf{w}_i^T\mathrm{e}^{-\overline{z}_i\tau_D} & \mathbf{0} & \cdots & \mathbf{0} & \overline{z}_i\mathbf{w}_i^T\mathrm{e}^{-\overline{z}_i\tau_F} & \mathbf{0} & \cdots & \mathbf{0} \\ \mathbf{0} & \overline{z}_i^2\mathbf{w}_i^T\mathrm{e}^{-\overline{z}_i\tau_D} & \cdots & \mathbf{0} & \mathbf{0} & \overline{z}_i\mathbf{w}_i^T\mathrm{e}^{-\overline{z}_i\tau_F} & \cdots & \mathbf{0} \\ \vdots & \vdots & \ddots & \vdots & \vdots & \vdots & \ddots & \vdots \\ \mathbf{0} & \mathbf{0} & \cdots & \overline{z}_i^2\mathbf{w}_i^T\mathrm{e}^{-\overline{z}_i\tau_D} & \mathbf{0} & \mathbf{0} & \cdots & \overline{z}_i\mathbf{w}_i^T\mathrm{e}^{-\overline{z}_i\tau_F} \end{bmatrix} \begin{Bmatrix} \widetilde{\mathbf{d}}_1 \\ \vdots \\ \widetilde{\mathbf{d}}_m \\ \widetilde{\mathbf{f}}_1 \\ \vdots \\ \widetilde{\mathbf{f}}_m \end{Bmatrix} = \begin{Bmatrix} \alpha_{i,1} \\ \vdots \\ \alpha_{i,m} \end{Bmatrix} \tag{31}$$

In a more compact form:

$$\boldsymbol{\Phi}_{\mathbf{dz},i}\widetilde{\mathbf{k}}_\mathbf{d} = \boldsymbol{\alpha}_{\mathbf{z},i} \tag{32}$$

Hence, similarly to Eq. (24), in the case of state-derivative feedback the control gains in the adjunct system are obtained by solving the assignment problem for n_z zeros:

$$\mathbf{\Phi_{dz}}\widetilde{\mathbf{k}}_\mathbf{d} = \boldsymbol{\alpha}_\mathbf{z} \tag{33}$$

In turn, matrices **D** and **F** are computed through the procedure outlined in Eq. (25).

3.2.2. The multi-step approach for the zero assignment in the state-derivative case

The multi-step approach is formulated with a similar mathematical formulation to the one proposed in Section 3.2.2 with obvious modifications. The counter part of Eq. (28) in the state-derivative case is:

$$\begin{bmatrix} \bar{z}_{1,k}^2 \mathbf{t}_{1,k}^T \mathrm{e}^{-\bar{z}_{1,k}\tau_D} & \bar{z}_{1,k} \mathbf{t}_{1,k}^T \mathrm{e}^{-\bar{z}_{1,k}\tau_F} \\ \bar{z}_{2,k}^2 \mathbf{t}_{2,k}^T \mathrm{e}^{-\bar{z}_{2,k}\tau_D} & \bar{z}_{2,k} \mathbf{t}_{2,k}^T \mathrm{e}^{-\bar{z}_{2,k}\tau_F} \\ \vdots & \vdots \\ \bar{z}_{n_z,k}^2 \mathbf{t}_{n_z,k}^T \mathrm{e}^{-\bar{z}_{n_z,k}\tau_D} & \bar{z}_{n_z,k} \mathbf{t}_{n_z,k}^T \mathrm{e}^{-\bar{z}_{n_z,k}\tau_F} \end{bmatrix} \begin{Bmatrix} \mathbf{f}_k \\ \mathbf{g}_k \end{Bmatrix} = \begin{Bmatrix} h_{pq,k-1}(\bar{z}_{1,k}) \\ h_{pq,k-1}(\bar{z}_{2,k}) \\ \vdots \\ h_{pq,k-1}(\bar{z}_{n_z,k}) \end{Bmatrix} \tag{34}$$

The demonstration for Eq. (34) can be inferred from Appendix A.

The linear system in Eq. (34) can be synthetized, with obvious meaning of the terms, as:

$$\mathbf{\Phi}_{\mathbf{dz},k}\mathbf{k}_{\mathbf{d},k} = \mathbf{y}_{\mathbf{z},k} \tag{35}$$

The control gain matrices **D** and **F** are obtained solving Eq. (35) for $k = 1, \ldots, m$.

3.3. Pole-zero placement by the receptance method: state feedback

3.3.1. Single-step: pole-zero placement through state feedback

The multi-input pole placement method exploiting receptances through a single-step approach has been introduced in the milestone paper [2] without including time-delay. Lately, it has been extended in [6] to account for delay, in the case of output feedback control. For brevity, we will just recall here the linear system for the assignment of n_p prescribed poles that belongs to the set $\sum_p = \left\{\bar{p}_1, \ldots, \bar{p}_{n_p}\right\}$. First, the i th pole $\bar{p}_i$ is assigned if:

$$\begin{bmatrix} \bar{p}_i\mathbf{v}_i^T\mathrm{e}^{-\bar{p}_i\tau_F} & \mathbf{0} & \cdots & \mathbf{0} & \mathbf{v}_i^T\mathrm{e}^{-\bar{p}_i\tau_G} & \mathbf{0} & \cdots & \mathbf{0} \\ \mathbf{0} & \bar{p}_i\mathbf{v}_i^T\mathrm{e}^{-\bar{p}_i\tau_F} & \cdots & \mathbf{0} & \mathbf{0} & \mathbf{v}_i^T\mathrm{e}^{-\bar{p}_i\tau_G} & \cdots & \mathbf{0} \\ \vdots & \vdots & \ddots & \vdots & \vdots & \vdots & \ddots & \vdots \\ \mathbf{0} & \mathbf{0} & \cdots & \bar{p}_i\mathbf{v}_i^T\mathrm{e}^{-\bar{p}_i\tau_F} & \mathbf{0} & \mathbf{0} & \cdots & \mathbf{v}_i^T\mathrm{e}^{-\bar{p}_i\tau_G} \end{bmatrix} \begin{Bmatrix} \mathbf{f}_1 \\ \vdots \\ \mathbf{f}_m \\ \mathbf{g}_1 \\ \vdots \\ \mathbf{g}_m \end{Bmatrix} = \begin{Bmatrix} \beta_{i,1} \\ \vdots \\ \beta_{i,m} \end{Bmatrix} \tag{36}$$

where:

$$\beta_{i,j} = \left(\bar{p}_i\mathbf{f}_j^T + \mathbf{g}_j^T\right)\mathbf{v}_i, \quad i = 1, \ldots, n_p \text{ and } j = 1, \ldots, m \tag{37}$$

and:

$$\mathbf{v}_i = \beta_{i,1}\mathbf{r}_{i,1} + \ldots + \beta_{i,m}\mathbf{r}_{i,m}, \quad i = 1, \ldots, m \tag{38}$$

with:

$$\mathbf{r}_{i,j} = \mathbf{H}(\bar{p}_i)\mathbf{b}_j, \quad i = 1, \ldots, n_p \text{ and } j = 1, \ldots, m \tag{39}$$

Such coefficients introduce some degrees of freedom in design, that allows optimizing the controller to satisfy secondary tasks (such as gain reduction [27] or the enforcement of modal constraints [2]). This issue goes beyond the goals of this paper, and will be the topic of our further investigation.

A more compact form for the linear system in Eq. (36) is: $\mathbf{\Phi}_{\mathbf{sp},i}\mathbf{k_s} = \boldsymbol{\beta}_{\mathbf{p},i}$, and for the assignment of n_p poles it yields:

$$\begin{bmatrix} \mathbf{\Phi}_{\mathbf{sp},1} \\ \vdots \\ \mathbf{\Phi}_{\mathbf{sp},n_p} \end{bmatrix} \mathbf{k_s} = \begin{Bmatrix} \boldsymbol{\beta}_{\mathbf{p},1} \\ \vdots \\ \boldsymbol{\beta}_{\mathbf{p},n_p} \end{Bmatrix} \tag{40}$$

In turn, Eq. (40) can be written as: $\mathbf{\Phi_{sp}}\mathbf{k_s} = \boldsymbol{\beta}_\mathbf{p}$.

The solution of the pole-zero placement problem is straightforward, i.e., the linear systems in Eqs.(24) and (40) are clustered together providing the linear system for the state feedback single-step multi-input pole zero placement:

$$\begin{bmatrix} \mathbf{\Phi}_{\mathbf{sz}}\mathbf{T} \\ \mathbf{\Phi}_{\mathbf{sp}} \end{bmatrix} \mathbf{k}_{\mathbf{s}} = \begin{Bmatrix} \boldsymbol{\alpha}_{\mathbf{z}} \\ \boldsymbol{\beta}_{\mathbf{p}} \end{Bmatrix} \tag{41}$$

with matrix $\mathbf{T} = \mathrm{blkdiag}\left(\mathbf{C}_{\mathbf{n}}^T, \dots, \mathbf{C}_{\mathbf{n}}^T\right)$. Since $\widetilde{\mathbf{k}}_{\mathbf{s}}$ is defined in the adjunct system, matrix $\mathbf{C}_{\mathbf{n}}^T$ is repeated 2 m times, i.e. the transformations in Eq. (25) are applied to obtain $\boldsymbol{k}_{\boldsymbol{s}}$.

3.3.2. Multi-step: state feedback pole-zero assignment

The multi-step method in Section 3.1.2 can be extended for the pole-zero assignment by considering the linear system proposed in [4,17] for the pole placement in the single input scenario. The path for the n_p prescribed poles $\sum_{p,k} = \left\{\overline{p}_{1,k}, \dots, \overline{p}_{n_p,k}\right\}$ should be defined similarly to the path defined for the zeros (see Section 3.1.2). Then, for the k-th step of the method, the n_p poles are assigned by solving the linear system:

$$\begin{bmatrix} \overline{p}_{1,k}\mathbf{r}_{1,k}^T e^{-\overline{p}_{1,k}\tau_F} & \mathbf{r}_{1,k}^T e^{-\overline{p}_{1,k}\tau_G} \\ \overline{p}_{2,k}\mathbf{r}_{2,k}^T e^{-\overline{p}_{2,k}\tau_F} & \mathbf{r}_{2,k}^T e^{-\overline{p}_{2,k}\tau_G} \\ \vdots & \vdots \\ \overline{p}_{n_p,k}\mathbf{r}_{n_p,k}^T e^{-\overline{p}_{n_p,k}\tau_F} & \mathbf{r}_{n_p,k}^T e^{-\overline{p}_{n_p,k}\tau_G} \end{bmatrix} \begin{Bmatrix} \mathbf{f}_k \\ \mathbf{g}_k \end{Bmatrix} = \begin{Bmatrix} 1 \\ 1 \\ \vdots \\ 1 \end{Bmatrix} \tag{42}$$

The updated receptance matrix $\overline{\mathbf{H}}_{k-1}(\overline{p}_i)$ and vector $\mathbf{r}_{i,k} = \overline{\mathbf{H}}_{k-1}(\overline{p}_i)\mathbf{b}_k$ are inferred from Eq. (26). A more compact notation for Eq. (42) is $\mathbf{\Phi}_{\mathbf{sp},k}\mathbf{k}_{\mathbf{s},k} = \mathbf{y}_{\mathbf{p},k}$. Eqs.(29) and (42) can be merged together to obtain the pole-zero placement problem for the k-th step:

$$\begin{bmatrix} \mathbf{\Phi}_{\mathbf{sz},k} \\ \mathbf{\Phi}_{\mathbf{sp},k} \end{bmatrix} \mathbf{k}_{\mathbf{s},k} = \begin{Bmatrix} \mathbf{y}_{\mathbf{z},k} \\ \mathbf{y}_{\mathbf{p},k} \end{Bmatrix} \tag{43}$$

Solving the k assignment problems in Eq. (43) for $k = 1, \dots, m$ yields the control gain matrices $\mathbf{F}$ and $\mathbf{G}$.

3.4. Pole-zero placement by the receptance method: state-derivative feedback

3.4.1. Single-step: pole-zero placement through state-derivative feedback

The solution for the assignment of n_p prescribed poles in the case of state-derivative feedback can be obtained by following the same procedure adopted to obtain Eq. (36) by considering Eq. (10) instead of Eq. (8). The linear system for the placement of the i th pole becomes:

$$\begin{bmatrix} \overline{p}_i^2\mathbf{v}_i^T e^{-\overline{p}_i\tau_D} & \mathbf{0} & \cdots & \mathbf{0} & \overline{p}_i\mathbf{v}_i^T e^{-\overline{p}_i\tau_F} & \mathbf{0} & \cdots & \mathbf{0} \\ \mathbf{0} & \overline{p}_i^2\mathbf{v}_i^T e^{-\overline{p}_i\tau_D} & \cdots & \mathbf{0} & \mathbf{0} & \overline{p}_i\mathbf{v}_i^T e^{-\overline{p}_i\tau_F} & \cdots & \mathbf{0} \\ \vdots & \vdots & \ddots & \vdots & \vdots & \vdots & \ddots & \vdots \\ \mathbf{0} & \mathbf{0} & \cdots & \overline{p}_i^2\mathbf{v}_i^T e^{-\overline{p}_i\tau_D} & \mathbf{0} & \mathbf{0} & \cdots & \overline{p}_i\mathbf{v}_i^T e^{-\overline{p}_i\tau_F} \end{bmatrix} \begin{Bmatrix} \mathbf{d}_1 \\ \vdots \\ \mathbf{d}_m \\ \mathbf{f}_1 \\ \vdots \\ \mathbf{f}_m \end{Bmatrix} = \begin{Bmatrix} \beta_{i,1} \\ \vdots \\ \beta_{i,m} \end{Bmatrix} \tag{44}$$

The right-hand side coefficients in Eq. (44) are $\beta_{i,j} = \left(\overline{p}_i^2\mathbf{d}_j^T + \overline{p}_i\mathbf{f}_j^T\right)\mathbf{v}_i, \quad i = 1, \dots, n_p$ and $j = 1, \dots, m$.

A similar approach to the one outlined in Section 3.3.1 is adopted to obtain the compact form $\mathbf{\Phi}_{\mathbf{dp}}\mathbf{k}_{\mathbf{s}} = \boldsymbol{\beta}_{\mathbf{p}}$. The linear system for the single-step pole-zero assignment through state-derivative feedback is obtained by merging Eqs.(33) and (44):

$$\begin{bmatrix} \mathbf{\Phi}_{\mathbf{dz}}\mathbf{T} \\ \mathbf{\Phi}_{\mathbf{dp}} \end{bmatrix} \mathbf{k}_{\mathbf{d}} = \begin{Bmatrix} \boldsymbol{\alpha}_{\mathbf{z}} \\ \boldsymbol{\beta}_{\mathbf{p}} \end{Bmatrix} \tag{45}$$

3.4.2. Multi-step: state-derivative feedback pole-zero assignment

In the case of the multi-step method Eq. (42) is adapted to the state-derivative scenario for the assignment of the n_p prescribed poles at the k-th step as follows:

$$\begin{bmatrix} \overline{p}_{1,k}^2\mathbf{r}_{1,k}^T e^{-\overline{p}_{1,k}\tau_D} & \overline{p}_{1,k}\mathbf{r}_{1,k}^T e^{-\overline{p}_{1,k}\tau_F} \\ \overline{p}_{2,k}^2\mathbf{r}_{2,k}^T e^{-\overline{p}_{2,k}\tau_D} & \overline{p}_{2,k}\mathbf{r}_{2,k}^T e^{-\overline{p}_{2,k}\tau_F} \\ \vdots & \vdots \\ \overline{p}_{n_p,k}^2\mathbf{r}_{n_p,k}^T e^{-\overline{p}_{n_p,k}\tau_D} & \overline{p}_{n_p,k}\mathbf{r}_{n_p,k}^T e^{-\overline{p}_{n_p,k}\tau_F} \end{bmatrix} \begin{Bmatrix} \mathbf{d}_k \\ \mathbf{f}_k \end{Bmatrix} = \begin{Bmatrix} 1 \\ 1 \\ \vdots \\ 1 \end{Bmatrix} \tag{46}$$

With a simplified notation: $\mathbf{\Phi}_{\mathbf{dp},k}\mathbf{k}_{\mathbf{d},k} = \mathbf{y}_{\mathbf{d},k}$. Finally, by clustering Eqs.(35) and (46), the linear system for the pole-zero assignment is obtained as follows:

$$\begin{bmatrix} \mathbf{\Phi}_{\mathbf{dz},k} \\ \mathbf{\Phi}_{\mathbf{dp},k} \end{bmatrix} \mathbf{k}_{\mathbf{d},k} = \begin{Bmatrix} \mathbf{y}_{\mathbf{z},k} \\ \mathbf{y}_{\mathbf{p},k} \end{Bmatrix} \tag{47}$$

The solution of Eq. (47) for $k = 1, \ldots, m$ yields the control gain matrices **D** and **F**.

3.5. Partial assignment

In several applications only a subset of dominant poles and zeros of interest must be assigned while the remaining are let free to arrange with some tolerance in the stable left-half of the complex plane [19,28]. In this scenario, if the number of required poles and zeros is smaller than 2 N, i.e. $n_p + n_z < 2N$, the linear system is underdetermined.

Let us generalize the linear systems in Eqs.(24), (29), (33), (35), (40), (43), (45), (47) through the following notation (with obvious meaning of the symbols in the different scenarios):

$$\mathbf{\Phi k} = \mathbf{y} \tag{48}$$

The solution $\boldsymbol{k}$ of Eq. (48), in the case of underdetermined linear system, is composed by two terms:

$$\mathbf{k} = \mathbf{k_0} + \mathbf{k_h} \tag{49}$$

$\boldsymbol{k_0}$ is the particular solution of the non-homogeneous equation, while $\boldsymbol{k_h}$ is a solution of the homogeneous system $\mathbf{\Phi k_h} = \mathbf{0}$. A common approach for computing $\boldsymbol{k_0}$ is through the Moore-Penrose pseudoinverse (denoted through †) [29] to minimize the norm of the control gains:

$$\mathbf{k} = \mathbf{\Phi}^{\dagger}\mathbf{y} \tag{50}$$

Alternatively, the weighted pseudoinverse [30] since measurements are dimensionally heterogeneous. Another approach to solve such linear system is through the QR-decomposition to force some entries of $\boldsymbol{k_0}$ to be equal to zero. The solution $\boldsymbol{k_0}$ ensures that the closed-loop system poles and zeros include the set of desired ones. However, it is not guaranteed that the controlled system is stable and robust with respect to uncertainties [14,19,31].

The set of all the possible solutions $\boldsymbol{k_h}$ can be conveniently parametrized through matrix **V**, whose columns spans the null space of $\mathbf{\Phi}$, and through the dimension-compatible real coefficients vector $\boldsymbol{k_r}$:

$$\mathbf{k} = \mathbf{k_0} + \mathbf{V k_r} \tag{51}$$

The term $\boldsymbol{k_h}$ can be exploited to satisfy secondary tasks, such as stabilizing the latent roots [13,14] and also increasing robustness. Indeed, in practical control applications, system parameters are uncertain, hence robustness should be addressed in the design phase.

In some recent works, efforts were made to incorporate in the design some *a priori* requisite to impose the closed-loop stability and pole clustering into prescribed regions of the complex plane through the LMI theory [14,31,32]. However, the method here proposed handles both the problems of control system design. Indeed, the chief idea of this paper is to exploit the space of all the possible homogeneous solutions $\boldsymbol{k_h}$ of Eq. (49) to obtain a stable closed-loop system with guaranteed prescribed robustness, by taking advantage of the generalized Nyquist contour.

4. Inclusion of stability and robustness constraints

4.1. Eigenloci: the generalized Nyquist contour

Papers [33] and [34] introduced the outstanding result that generalizes the concept of Nyquist contour of a SISO system (single input, single output) to systems with multiple inputs and outputs. Consider again the system in Eq. (1) under the feedback control in Eqs.(8) or (10), with the controller transfer function $\mathbf{\Theta}(s)$ equal to

$$\mathbf{\Theta}(s) = \mathbf{F}^T e^{-\tau_F s} s + \mathbf{G}^T e^{-\tau_G s} \tag{52}$$

in case of state feedback, or equal to

$$\mathbf{\Theta}(s) = \mathbf{D}^T e^{-\tau_D s} s^2 + \mathbf{F}^T e^{-\tau_F s} s \tag{53}$$

in the case of state-derivative feedback.

The closed-loop receptance of such a system can be written as:

$$\overline{\mathbf{H}}(s) = \left[\mathbf{M}s^2 + \mathbf{C}s + \mathbf{K} - \mathbf{B}\Theta(s)\right]^{-1} \tag{54}$$

By applying the matrix inversion lemma [35] to Eq. (54) it is possible to relate the receptance of the open and closed loop systems as follows:

$$\overline{\mathbf{H}}(s) = \mathbf{H}(s) + \mathbf{H}(s)\mathbf{B}[\mathbf{I} - \mathbf{\Theta}(s)\mathbf{H}(s)\mathbf{B}]^{-1}\mathbf{H}(s) \tag{55}$$

Using the loop function concept [17], the closed-loop poles can be computed using the characteristic equation of Eq. (55), i.e.:

$$\det[\mathbf{I} + \mathbf{L}(s)] = 0 \tag{56}$$

in which $\mathbf{L}(s) = -\boldsymbol{\Theta}(s)\mathbf{H}(s)\mathbf{B}$ is the loop gain function. Now, let us set $s = \mathrm{i}\omega$, with $\mathrm{i} = \sqrt{-1}$ and ω is the frequency, and let us introduce the following definitions and assumption.

Definition 1. The *eigenloci* is the set of all the geometric branches, in the complex plane, obtained by computing the eigenvalues $\lambda_j[\mathbf{L}(\mathrm{i}\omega)] \in \mathbb{C}$, $j = 1, \ldots, m$ for all the frequencies $\omega \in \boldsymbol{\Omega}$ (which is the discrete set of frequencies belonging to the range of interest $0 \le \omega_{\mathrm{inf}} < \omega_{\mathrm{sup}} \le \omega_{\mathrm{Nyq}}$, with ω_{Nyq} is the Nyquist frequency of the control loop).

Definition 2. The number of counterclockwise encirclements of the point $-1 + 0\mathrm{i}$ by the k-th branch of the eigenloci in the complex plane is denoted by $c_e\{\lambda_k[\mathbf{L}(\mathrm{i}\omega)]\}$.

Definition 3. The number of clockwise encirclements of the point $-1 + 0\mathrm{i}$ by the k-th branch of the eigenloci in the complex plane is denoted by $c_e^c\{\lambda_k[\mathbf{L}(\mathrm{i}\omega)]\}$.

Assumption 1. The loop function $\mathbf{L}(\mathrm{i}\omega)$ has no clockwise encirclements of the critical point $-1 + 0\mathrm{i}$, that is, $\sum_{k=1}^{m} c_e^c\{\lambda_k[\mathbf{L}(\mathrm{i}\omega)]\} = 0$.

The cornerstone result from [34] is given by the following Lemma:

Lemma 1. *The closed-loop system in Eq. (54) with Assumption 1 is exponentially stable iff:*

(a) $-1 + 0\mathrm{i} \notin \lambda_j[\mathbf{L}(\mathrm{i}\omega)]$, $j = 1, \ldots, m$;
(b) $\sum_{k=1}^{m} c_e\{\lambda_k[\mathbf{L}(\mathrm{i}\omega)]\} = p_+^0$, where p_+^0 is the number of open-loop poles that belong to the complex right-half plane.

4.2. System margins and robustness

This paper exploits the interesting approach of the disk margin constraint to Nyquist contours [36] to guarantee *a priori* stability and the prescribed robustness solving the problems introduced in Section 3.5. The approach is based on the following chief idea: since the closed loop stability is preserved as long as the number of counterclockwise encirclements of $-1 + 0i$ does not change, then enforcing the eigenloci outside a disk of radius M_s centered at the critical point gives the following minimum guaranteed gain margin GM and phase margin PM to open-loop stable systems [37]:

$$GM \ge \frac{M_s}{M_s - 1}, \quad PM \ge 2\sin^{-1}\left(\frac{1}{2M_s}\right) \tag{57}$$

In the case of unstable open-loop systems, since that counter clockwise encirclements must exist, the closed-loop system shall have a range for the gain and phase perturbations [38] defined by the intervals $[GM^-, GM^+]$ and $[PM^-, PM^+]$, with:

$$\begin{aligned} &GM^+ \ge \frac{M_s}{M_s - 1}, \quad PM^+ \ge 2\sin^{-1}\left(\frac{1}{2M_s}\right) \\ &GM^- \le \frac{M_s}{M_s + 1}, PM^- \le -2\sin^{-1}\left(\frac{1}{2M_s}\right) \end{aligned} \tag{58}$$

4.3. Pole-zero assignment with guaranteed robustness

By exploiting Theorem 1, together with the related results discussed in Section 4.2, and the parametrization of the gain vector ensuring pole-zero placement, discussed in Section 3, $\boldsymbol{k_r}$ is computed by solving the following minimization problem to obtain a stable closed-loop system with guaranteed prescribed robustness:

$$\begin{aligned} &\min_{\mathbf{k_r}} \quad h(\mathbf{k_r}) = \left(\inf_{\omega_j} \left|\lambda_k\left[\mathbf{L}(\mathrm{i}\omega_j)\right] + 1\right| - M_s^{-1}\right)^2 \\ &\text{s.t.} \begin{cases} \sum_{k=1}^{m} c_e^c\{\lambda_k[\mathbf{L}(\mathrm{i}\omega)]\} = 0 \\ \sum_{k=1}^{m} c_e\{\lambda_k[\mathbf{L}(\mathrm{i}\omega)]\} = p_+^0 \\ \mathbf{k} = \mathbf{k_0} + \mathbf{V}\mathbf{k_r} \\ \omega_j \in \boldsymbol{\Omega} \end{cases} \end{aligned} \tag{59}$$

$\mathbf{L}(\mathrm{i}\omega)$ is a function of the decision variable $\boldsymbol{k_r}$ and in the case of state-feedback control is formulated as follows:

$$\mathbf{L}(\mathrm{i}\omega) = -(\mathrm{i}\omega\mathbf{F} + \mathbf{G})\mathbf{H}(\mathrm{i}\omega)\mathbf{B} \tag{60}$$

In contrast, in the state-derivative control is:

$$\mathbf{L}(\mathrm{i}\omega) = -\left(\mathrm{i}\omega\mathbf{F} - \omega^2\mathbf{D}\right)\mathbf{H}(\mathrm{i}\omega)\mathbf{B} \tag{61}$$

It should be noted that Eq. (59), in principle, could be formulated equivalently as a minimization with respect to $\boldsymbol{k}$ instead of $\boldsymbol{k_r}$ by including in the set of constraints also Eq. (48), i.e., $\mathbf{\Phi k} = \mathbf{y}$. However, since the dimension of $\boldsymbol{k_r}$ is $2Nm\text{-}(n_p{+}n_z)$ while $\boldsymbol{k}$ size is $2Nm$, formulating the problem as done in Eq. (59) reduces the number of unknowns and then improves the numerical convergence of the genetic algorithm.

4.4. Numerical implementation of the genetic algorithm

The solution method here proposed is achieved using the techniques of evolutional algorithms ([17,39]) thanks to its reliability and simplicity of implementation. It is worth noticing that the proposed method handles both receptance-based formulation (i.e., when experimental or numerical $\mathbf{H}(s)$ is available) and model representations based on the **M, C, K** system matrices.

The algorithm can be summarized through the steps listed in Table 1.

The individuals of the population in the search algorithm are generated using Eq. (51) in the search space for $\boldsymbol{k_r}$. The next step is the evaluation of the solution candidates, and it is done through the robustness index related to the M_s disk as in [16,17]. The so-called fitness function is adopted as the cost function in Eq. (59). This is referred to the shortest distance between the eigenloci and the critical point once it is kept in a tangent point on the circumference of the M_s disk. The quadratic form of the fitness function indicates that one can achieve the minimum when the first term is equal to the second, which means that the related individual gives an eigenloci that touches the boundary of the disk from outside.

The constraint function, as well as the fitness function, is based on Theorem 1, with an additional penalization term as:

$$C = \left(\min\{X_c\}\sum_{k=1}^{m} c_e^c\{\lambda_k[\mathbf{L}(\mathrm{i}\omega)]\} + p_+^0 - \sum_{k=1}^{m} c_e\{\lambda_k[\mathbf{L}(\mathrm{i}\omega)]\}\right)^2 \tag{62}$$

where $\min\{X_c\}$ is the minimum value of the vector X_c that stores the values of the point that crosses the real axis. This minimum indicates the fartherst point of the eigenloci from the critical point $-1+0\mathrm{i}$ by its left side. c_e^c is the number of clockwise encirclements of the critical point by the k-th branch of eigenloci, with $\sum_{k=1}^{m} c_e^c\{\lambda_k[\mathbf{L}(\mathrm{i}\omega)]\}$ being the total number of clockwise encirclements; $c_e$and p_+^0 have been defined in Section 4.1.

As in the fitness function the quadratic form indicates stability when C equals zero. In this scenario there are no encirclements in the clockwise direction, that is, $\sum_{k=1}^{m} c_e^c\{\lambda_k[\mathbf{L}(\mathrm{i}\omega)]\} = 0$, and $\sum_{k=1}^{m} c_e\{\lambda_k[\mathbf{L}(\mathrm{i}\omega)]\} = p_+^0$. On the other hand, when $C \neq 0$, for evolution of the search, the individual must have an evaluation that points to the way of stability and that is the role played by the vector X_C. Thus, unstable individuals have distinct values for the constraint based on the distance of the crossings by the left size of the critical point; the shorter is the distance the nearest to achieving stability the system is.

5. Numerical assessment

5.1. Examples overview

In the next Sections, the effectiveness and the relevance of the proposed methods with respect to the actual state-of-the-art will be demonstrated through the application to some meaningful test-cases taken from the existing literature. A summary of the test-cases proposed is provided in Table 2.

The correctness of the assignment in the examples is assessed by evaluating the value of the closed-loop receptance for the desired zeros while, for the desired poles the value of the determinant is calculated (p_k denotes a pole to be assigned).

Stability is assessed by verifying that the dominant and latent roots lie in the left-half of the complex plane, i.e. their real part is

Table 1
Summary of the genetic algorithm.

Searching Algorithm – State or State-Derivative Feedback Gains Computation	
Inputs: $\mathbf{M}, \mathbf{C}, \mathbf{K}, \mathbf{B}$ - or $\mathbf{H}(s)$, $\mathbf{B}$, τ_F, τ_G - or τ_D, $\mathbf{k}_0, \mathbf{V}, M_s, p_0^+, \omega, \boldsymbol{\Omega}$ Output: k_r	
1	**Function** GAsearch:
2	**Create** an *Initial Population* of vectors $\boldsymbol{k_r}$;
3	**Evaluate** all individuals created in step 2 according to the fitness function and the constraints
4	**If** the best individual satisfies the objective function and constraints;
5	***Return*** *Best-Individual;*
6	**End**
7	**Create** a *new-population* of $\boldsymbol{k_r}$ Crossing the individuals in actual population;
8	**Evaluate** the new individuals;
9	**Return** to Step 4

Table 2
Summary of the four test-cases.

Test case section	5.2	5.3	5.4	5.6
System matrices	**M, C, K** Symmetric	**M** Symmetric **C, K** Asymmetric	**M, C** Symmetric **K** Asymmetric	**M, C, K** Symmetric
Number of DOFs	3	3	2	4
Number of p_+^0	0	2	2	0
Number of assigned zeros	1 complex conjugate pair	1 complex conjugate pair	1 complex conjugate pair	1 complex conjugate pair
Number of assigned poles	–	1 complex conjugate pair	–	–
Point/Cross receptance	Point-receptance	Cross-receptance	Point-receptance	Cross-receptance
Solution methods tested	Single-step	Single-step	Single-step Multi-step	Single-step
Type of feedback	State State-derivative	State	State State-derivative	State

negative. The closed-loop system stability is further assessed by simulating its free response. Lastly, the fulfillment of the robustness requirement is evaluated by representing the eigenloci of the closed-loop system and verifying that its curve remains outside the circle of radius M_s.

5.2. Test-case 1 - Three masses: single step zero assignment

In this test-case, a three masses example borrowed from [6,14] is considered to study the effectiveness of the proposed approach through the single-step approach. The system matrices are:

$$\mathbf{M} = \begin{bmatrix} 2 & 0 & 0 \\ 0 & 2 & 0 \\ 0 & 0 & 3 \end{bmatrix}, \quad \mathbf{C} = \begin{bmatrix} 2.5 & -2 & 0 \\ -2 & 3 & -1 \\ 0 & -1 & 1 \end{bmatrix}, \quad \mathbf{K} = \begin{bmatrix} 10 & -3 & -4 \\ -3 & 3 & 0 \\ -4 & 0 & 4 \end{bmatrix}, \quad \mathbf{B} = \begin{bmatrix} 1 & 2 \\ 2 & 0 \\ 1 & 1 \end{bmatrix} \tag{63}$$

The time-delays are: $\tau_F = 0.2$ s and $\tau_G = 0.1$ s. The goal of control is to assign two closed-loop complex conjugate pairs of zeros $\Sigma_z = \{\pm \mathrm{i}, \ -0.5 \pm 2\mathrm{i}\}$ for point-receptance h_{11}. Additionally, it is required $M_s = 2.5$.

The coefficients in Eq. (18) and collected in vector $\boldsymbol{\alpha}_{\mathbf{z}} = \begin{bmatrix} \boldsymbol{\alpha_1}^T & \boldsymbol{\alpha_2}^T & \boldsymbol{\alpha_3}^T & \boldsymbol{\alpha_4}^T \end{bmatrix}^T$ are randomly chosen, resulting in:

$$\boldsymbol{\alpha}_1 = \alpha_2^* = \begin{bmatrix} 0.1418 + 0.0196\mathrm{i} \\ 1.7593 + 0.4274\mathrm{i} \end{bmatrix}, \boldsymbol{\alpha}_3 = \alpha_4^* = \begin{bmatrix} -1.0438 - 0.7460\mathrm{i} \\ -0.0554 + 0.4998\mathrm{i} \end{bmatrix} \tag{64}$$

5.2.1. Example 1: state feedback

The initial state feedback gains $\boldsymbol{k_0}$ computed with Eq. (24), through the *pinv* function in MATAB, are listed in Table 3. The assignment of the antiresonance is exactly fulfilled with this solution, as shown through the poles and zeros listed in Table 4. However, some unstable closed-loop poles are obtained.

To correct the solution by means of the term $\mathbf{Vk_r}$, a search for the robust final gains was performed with $M_s = 2.5$, leading to the gains listed in Table 3. Since the system is open-loop stable, i.e., $p_+^0 = 0$, no encirclement of the point $-1 + 0\mathrm{i}$ exists in the eigenloci displayed in Fig. 2. Further, the eigenloci of the unstable solution $\boldsymbol{k_0}$ is compared with the robust one in Fig. 3, which evidences that the solution based on genetic algorithm enables to increase the stability margins of the system, since the eigenloci with $\boldsymbol{k}$ is completely outside the safety disk.

The free-evolutions of the controlled system with initial conditions $\boldsymbol{x}(0) = [1 \quad 0 \quad 0]^T, \dot{\boldsymbol{x}}(0) = \mathbf{0}$ are shown in Fig. 4, which corroborates that the closed-loop stability is achieved with $\boldsymbol{k}$, while the response of the system controlled with $\boldsymbol{k_0}$ diverges. Fig. 5 shows the zero map of the closed-loop receptance $\overline{h}_{11}$ computed by exploiting the DDE-BIFTOOL package [9]. Finally, the fulfilment of the assignment task is further certified by the negligible values of the receptances evaluated at the prescribed zeros, indeed $\overline{h}_{11}(\pm \mathrm{i}) = (-7.0 \mp 2.5\mathrm{i})e - 17$ and $\overline{h}_{11}(-0.5 \pm 2\mathrm{i}) = (-1.2 \pm 9.1\mathrm{i})e - 16$.

Table 3
Example 1: control gains.

Non robust control (k_0)	Robust control (k)
$\mathbf{F}_0 = \begin{bmatrix} 0 & 0 \\ 0.3341 & 0.6897 \\ 0.1547 & 0.4725 \end{bmatrix}$	$\mathbf{F} = \begin{bmatrix} -0.9851 & -0.9378 \\ 0.3341 & 0.6897 \\ 0.1547 & 0.4725 \end{bmatrix}$
$\mathbf{G}_0 = \begin{bmatrix} 0 & 0 \\ -3.7288 & 0.0771 \\ 1.3412 & 0.8543 \end{bmatrix}$	$\mathbf{G} = \begin{bmatrix} -0.2720 & -0.0283 \\ -3.7288 & 0.0771 \\ 1.3412 & 0.8543 \end{bmatrix}$

Table 4
Receptance h_{11}: dominant open-loop and closed-loop zeros and system poles in example 1.

	Gains with k_0	Robust control gains k
Open-loop zeros	**Closed-loop zeros**	**Closed-loop zeros**
$-0.1029 \pm 1.1567i$	$\pm i$	$\pm i$
$-0.8137 \pm 0.9061i$	$-0.5 \pm 2i$	$-0.5 \pm 2i$
Open-loop poles	**Closed-loop poles**	**Closed-loop poles**
$-0.0305 \pm 0.5894i$	$0.0472 \pm 0.5204i$	$-0.2475 \pm 0.5254i$
$-0.0903 \pm 1.0119i$	$-0.1383 \pm 1.9188i$	$-0.4552 \pm 2.0677i$
$-0.6609 \pm 2.1200i$	$-1.0986 \pm 2.1457i$	$-1.1964 \pm 2.1882i$

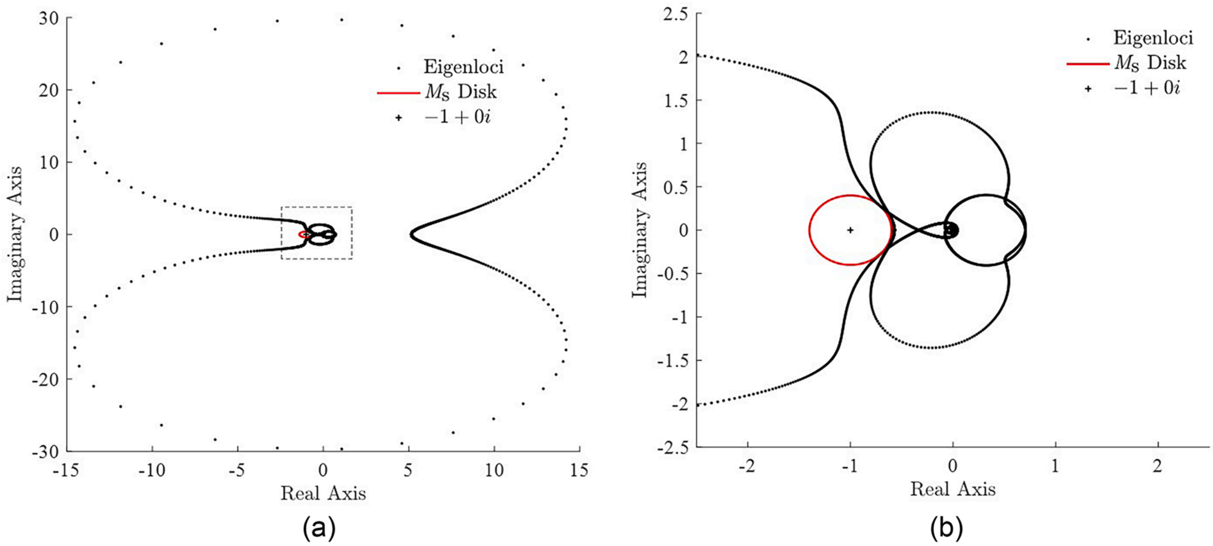

Fig. 2. The eigenloci of the system in example 1: (a) Full view; (b) Magnified view.

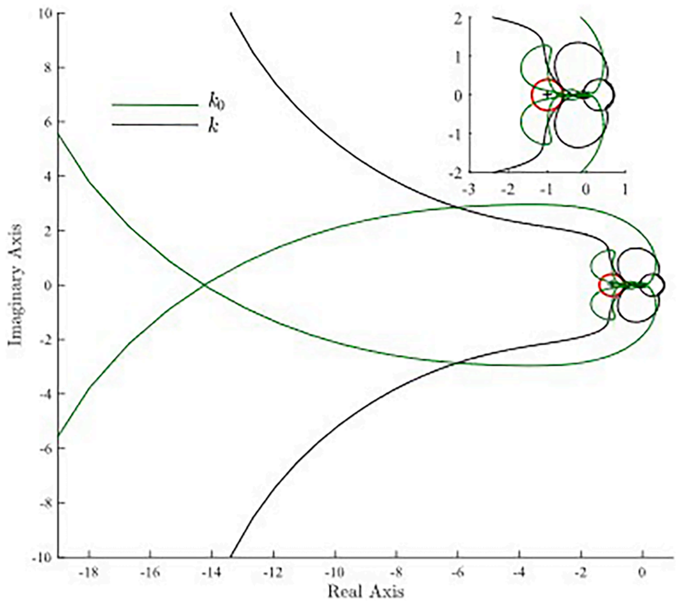

Fig. 3. Eigenloci with k_0 and with k.

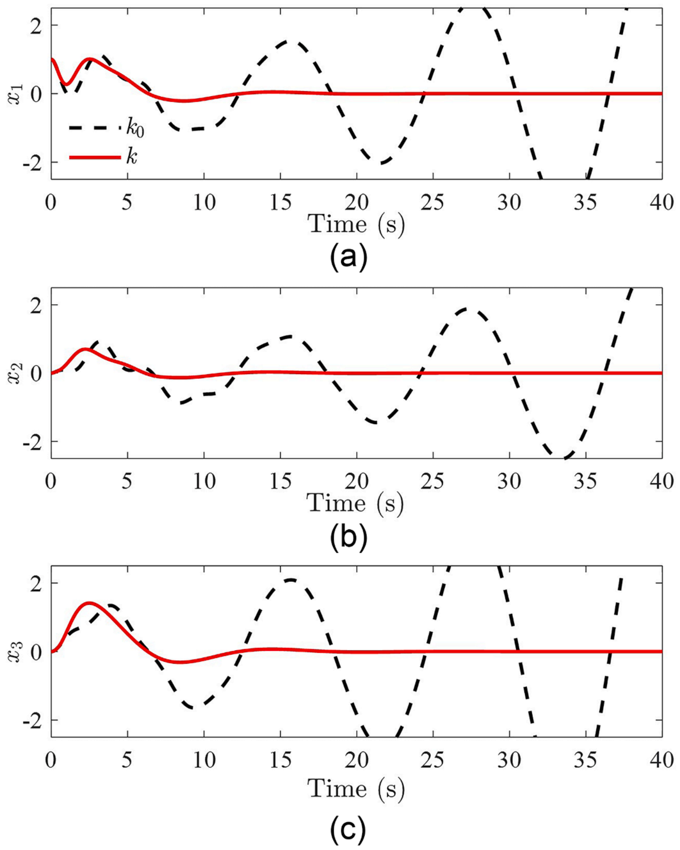

Fig. 4. Free-evolution of the closed-loop system in example 1 with k_0 (black dashed line) and with k (red line), coordinate displacements: x_1 (a), x_2 (b), x_3 (c).

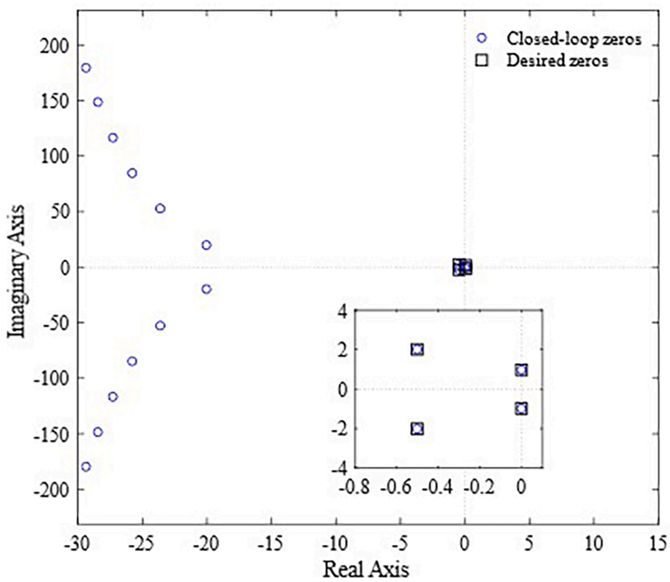

Fig. 5. Map of the zeros of the closed-loop receptance h_{11} for example 1.

5.2.2. Example 2: state-derivative feedback

The state-derivative controller has been also designed to cope with the same assignment task, and with the time delay on the acceleration feedback $\tau_D = 0.1$ s. The target assignment has been successfully achieved with the gains summarized in Table 5.

Again, an unstable initial design in case of $\boldsymbol{k_0}$ is obtained as corroborated by the positive real part closed-loop poles listed in Table 6. The eigenloci search is performed, with the final gains $\boldsymbol{k}$ resulting in the eigenloci of Fig. 6. The final gains obtained are summarized in Table 5. The correctness of the assignment is corroborated by the low values of the receptance at the prescribed zeros $\overline{h}_{11}(\pm \mathrm{i}) = (0.7 \mp 1.8\mathrm{i})e - 16$ and $\overline{h}_{11}(-0.5 \pm 2\mathrm{i}) = (-9.3 \mp 0.1\mathrm{i})e - 17$.

5.3. Test-case 2 - Flutter Control of a wing in an Airstream: pole-zero assignment

This is a classical benchmark problem taken from the literature whose matrices models the unstable vibrations (flutter) of a wing that travels in an airstream [32,40,41]. The system matrices are:

$$\mathbf{M} = \begin{bmatrix} 17.6 & 1.28 & 2.89 \\ 1.28 & 0.824 & 0.413 \\ 2.89 & 0.413 & 0.725 \end{bmatrix}, \ \mathbf{C} = \begin{bmatrix} 7.66 & 2.45 & 2.1 \\ 0.23 & 1.04 & 0.223 \\ 0.6 & 0.756 & 0.658 \end{bmatrix}, \ \mathbf{K} = \begin{bmatrix} 121 & 18.9 & 15.9 \\ 0 & 2.7 & 0.145 \\ 11.9 & 3.64 & 15.5 \end{bmatrix}, \ \mathbf{B} = \begin{bmatrix} 1 & 0 \\ 0 & 1 \\ 0 & 0 \end{bmatrix} \tag{65}$$

Time delays in velocity and displacement measurements are $\tau_F = 0.1$ s and $\tau_G = 0.05$ s. The state-derivative feedback design is not considered in this test-case for brevity.

Differently from the test-case 1 in Section 5.2 this system is open-loop unstable due to the positive real part complex conjugate eigenpair $\lambda_{1,2} = 0.0947 \pm 2.5229\mathrm{i}$ as reported in Table 8. The design aims to assign to the closed-loop system a pair of complex conjugate zeros $\Sigma_z = \{\pm 5\mathrm{i}\}$ for cross-receptance h_{21} and two poles $\Sigma_p = \{-1 \pm \mathrm{i}\}$. A disk for robust margins is considered with $M_s = 2.5$. Again, the modal vector coefficients $\boldsymbol{\alpha}_\mathbf{z}$ and $\boldsymbol{\beta}_\mathbf{p}$ are randomly chosen, resulting in:

$$\boldsymbol{\alpha}_\mathbf{z} = \begin{bmatrix} 0.4889 + 0.7269\mathrm{i} \\ 1.0347 - 0.3034\mathrm{i} \\ 0.4889 - 0.7269\mathrm{i} \\ 1.0347 + 0.3034\mathrm{i} \end{bmatrix}, \boldsymbol{\beta}_\mathbf{p} = \begin{bmatrix} 0.2939 + 0.8884\mathrm{i} \\ -0.7873 - 1.1471\mathrm{i} \\ 0.2939 + 0.8884\mathrm{i} \\ -0.7873 + 1.1471\mathrm{i} \end{bmatrix} \tag{66}$$

5.3.1. Example 3: state feedback

The solution $\boldsymbol{k_0}$ of the pole-zero assignment problem obtained by solving the linear system in Eq. (24) through the *pinv* function yields the control gains listed in Table 7. The fulfillment of the assignment task is corroborated by the poles and the zeros reported in Table 8. The closed-loop poles obtained with $\boldsymbol{k_0}$ even though correctly assigned yield an unstable system.

Robustness and stability is achieved by requiring a disk for robust margins with $M_s = 2.5$; Fig. 7 shows the eigenloci of the closed-loop system with the gains $\boldsymbol{k}$ (reported in Table 7) obtained after the application of the genetic algorithm. The eigenloci features $p_+^0 = 2$ encirclements of the point $-1 + 0\mathrm{i}$. The free-evolutions of the closed-loop system from the initial conditions $\boldsymbol{x}(0) = [0.1 \quad 0 \quad 0]^T$, $\dot{\boldsymbol{x}}(0) = \mathbf{0}$ are displayed in Fig. 8 for both the closed-loop systems with $\boldsymbol{k_0}$ and $\boldsymbol{k}$. The achievement of the system stability with $\boldsymbol{k}$ and the correctness of the pole-zero assignment is corroborated by the eigenvalues reported in Table 8 and through the pole-zero map in Fig. 9.

5.3.2. Example 4: margins from the eigenloci

Let us consider the eigenloci in Fig. 7. One can compute the stability margins following the rule that the encirclements of the critical point cannot change to assure the closed-loop stability [42]. The block scheme adopted to test the stability margins is depicted in Fig. 10, in which $\boldsymbol{\Delta} = \delta \mathbf{I}$ with $\delta \in \mathbb{R}$being the static gain change; and $\gamma \in \mathbb{R}^+$is an incremental delay in the loop. In an uncertainty free scenario, one has $\delta = 0$ and $\gamma = 0$. Two gain margins are observed from the crossings with the real axis, and these two were computed as the upper gain margin $GM^+ = 1.8182$ and the lower gain margin $GM^- = 0.1471$, while the delay margin $DM = 0.4715$ is computed using the angle of the complex number given by the intersection of the eigenloci with the unitary circumference centered at the origin. The system was simulated using one by one these margins in the loop, and the results are displayed in Fig. 11. The responses are marginally stable, and this corroborates the system stability margins taken from the resulting eigenloci.

Table 5
Example 2: control gains.

Non robust control (k_0)	Robust control (k)
$\mathbf{F}_0 = \begin{bmatrix} 0 & 0 \\ 0.7484 & 0.4320 \\ -0.6497 & 2.1131 \end{bmatrix}$	$\mathbf{F} = \begin{bmatrix} -1.9579 & -1.3166 \\ 0.7484 & 0.4320 \\ -0.6497 & 2.1131 \end{bmatrix}$
$\mathbf{D}_0 = \begin{bmatrix} 0 & 0 \\ 0.7173 & -0.0369 \\ 0.0436 & -0.65136 \end{bmatrix}$	$\mathbf{D} = \begin{bmatrix} -1.6318 & 0.0960 \\ 0.7173 & -0.0369 \\ 0.0436 & -0.6513 \end{bmatrix}$

Table 6
Receptance h_{11}: dominant open-loop and closed-loop zeros and system poles in example 2.

	Gains with k_0	Robust control gains k
Open-loop zeros	**Closed-loop zeros**	**Closed-loop zeros**
$-0.1029 \pm 1.1567i$	$\pm i$	$\pm i$
$-0.8137 \pm 0.9061i$	$-0.5 \pm 2i$	$-0.5 \pm 2i$
Open-loop poles	**Closed-loop poles**	**Closed-loop poles**
$-0.0305 \pm 0.5894i$	$0.4494 \pm 0.3448i$	$-0.0704 \pm 0.4022i$
$-0.0903 \pm 1.0119i$	$-0.2576 \pm 1.4657i$	$-0.4975 \pm 1.2936i$
$-0.6609 \pm 2.1200i$	$-1.3170 \pm 2.7490i$	$-2.1014 \pm 4.7238i$

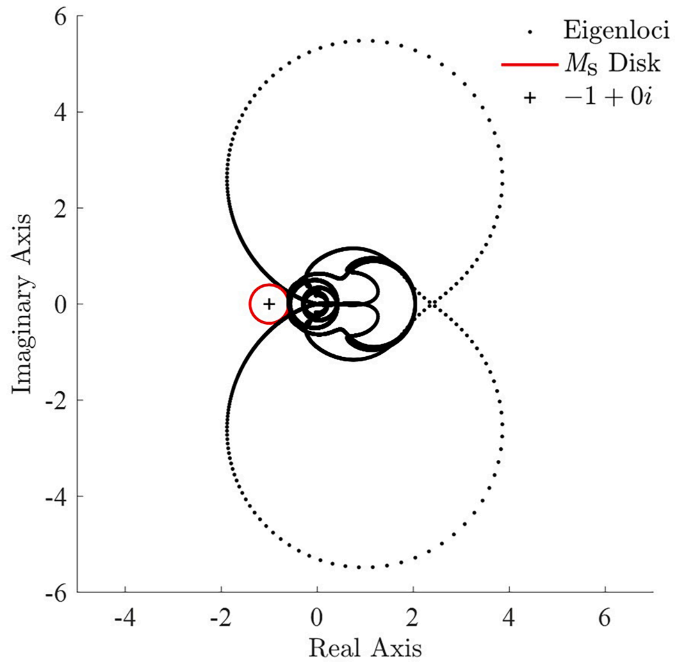

Fig. 6. The eigenloci of the system in example 2.

Table 7
Example 3: control gains.

Non robust control (k_0)	Robust control (k)
$\mathbf{F}_0 = \begin{bmatrix} -0.4430 & 1.9645 \\ -0.2725 & -0.0830 \\ -1.4833 & -0.5084 \end{bmatrix}$	$\mathbf{F} = \begin{bmatrix} -5.7239 & 1.6175 \\ -0.9183 & -0.5650 \\ -1.6449 & -0.3649 \end{bmatrix}$
$\mathbf{G}_0 = \begin{bmatrix} 0.0446 & 0.3047 \\ -0.9195 & 0.6576 \\ 1.7955 & -7.0899 \end{bmatrix}$	$\mathbf{G} = \begin{bmatrix} -1.4798 & -14.0565 \\ -0.9604 & -1.8103 \\ 0.2817 & -8.0369 \end{bmatrix}$

5.4. Test-case 3: multi-step zero assignment

In this test-case, the zero assignment multi-step method described in Sections 3.1.2 for state feedback and 3.2.2 for the state-derivative scenario is applied using the asymmetric model studied by Shapiro in [43] that can be associated to the operation of robotic grasping The system matrices are:

$$\mathbf{M} = \begin{bmatrix} 10 & 0 \\ 0 & 11 \end{bmatrix}, \qquad \mathbf{C} = \begin{bmatrix} 4 & 1 \\ 1 & 5 \end{bmatrix}, \qquad \mathbf{K} = \begin{bmatrix} 8 & 4 \\ -4 & 9 \end{bmatrix} \tag{67}$$

The actuation matrix is $\mathbf{B} = \begin{bmatrix} 1 & -1 \\ 0 & 1 \end{bmatrix}$. Mechanical contacts in this kind of systems yields an asymmetric stiffness matrix which in turn yields the following open loop poles: $\lambda_{1,2} = 0.004 \pm 0.9i$, $\lambda_{3,4} = -0.431 \pm 0.9i$, Hence, the first eigenvalue pair express the

Table 8
Receptance h_{21}: dominant open-loop and closed-loop zeros and system poles in example 3.

	Gains with k_0	Robust control gains k
Open-loop zeros	**Closed-loop zeros**	**Closed-loop zeros**
$-0.3700 \pm 5.2349i$	$-1.0132 \pm 10.0142i$	3.1590
$-0.6748 \pm 1.7492i$	$\pm 5i$	$\pm 5i$
Open-loop poles	**Closed-loop poles**	**Closed-loop poles**
$0.0947 \pm 2.5229i$	$-0.0074 \pm 2.6192i$	$-0.5591 \pm 2.9255i$
$-0.8848 \pm 8.4415i$	$-0.3044 \pm 7.2765i$	$-0.5713 \pm 7.6040i$
$-0.9180 \pm 1.7606i$	$-1 \pm 1i$	$-1 \pm 1i$

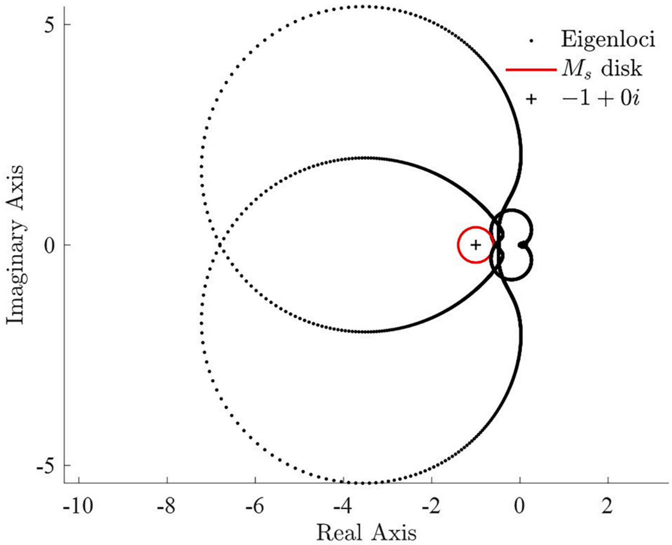

Fig. 7. The eigenloci of the system in example 3.

instability of the open-loop system. The goal of this example is to stabilize the closed-loop system while simultaneously assigning the pair of zeros that belongs to the set $\Sigma_z = \{\pm i\}$ for the driving-point receptance $\overline{h}_{22}$. Additionally, robustness is required by setting $M_s = 2$. The following time delays are assumed: $\tau_F = 0.2$ and $\tau_G = 0.5$ for the state feedback design while $\tau_D = 0.5$ for the state-derivative one. In the following subsections, the corresponding designs are explored.

5.4.1. Example 5: state feedback

The multi-step zero assignment is here solved for $k = 1, 2$ since rank$(\mathbf{B}) = 2$. In this example, the controller is tuned by using the GA search after all steps to obtain stable closed-loop systems at each of the steps. This approach is suitable to make the system fault tolerant to failures of the actuator considered in the last step of the placement path. Therefore, the sequency of steps should be done by ordering the actuators with a decreasing reliability, and hence by considering the most prone to fail as the very last step of the assignment.

Fig. 12 shows the eigenloci after each step. The control gains obtained are: $\mathbf{F} = \begin{bmatrix} 1.3417 & -1.3291 \\ 7.7543 & -1.0002 \end{bmatrix}$, $\mathbf{G} = \begin{bmatrix} -1.2393 & 1.6443 \\ 10.3494 & -0.1950 \end{bmatrix}$. The correctness of the antiresonance assignment is confirmed by: $\overline{h}_{22}(\pm i) = (-9.9 \mp 0.25i)e - 18$.

A comparison of the multi-step method against the single-step method is hereafter provided to highlight the capability of the controller to ensure robust stability with respect to failure of the second actuator. The same zero assignment and robustness specifications are required for the single-step method and the gains obtained are: $\mathbf{F}_s = \begin{bmatrix} -0.5869 & -3.2577 \\ -11.0594 & -38.1870 \end{bmatrix}$, $\mathbf{G}_s = \begin{bmatrix} -3.2856 & -0.4020 \\ -15.6002 & -35.8337 \end{bmatrix}$, assuming $\boldsymbol{\alpha}_{\mathbf{z},1} = \boldsymbol{\alpha}^*_{\mathbf{z},2} = \begin{bmatrix} -1+i \\ -1-i \end{bmatrix}$.

Table 9 displays the dominant eigenvalues of the system with no fault and with a failure in the second actuator (i.e., $k = 2$). Fig. 13 displays the free response of both systems with a failure in the mentioned actuator. As expected, the multi-step design is robust (indeed there are no poles with positive real part), while the single step design is not since this occurrence cannot be handled in design. It is worth noticing that the same instability issue may be experienced if the multi-step approach is used and the GA is applied at once after the last assignment step.

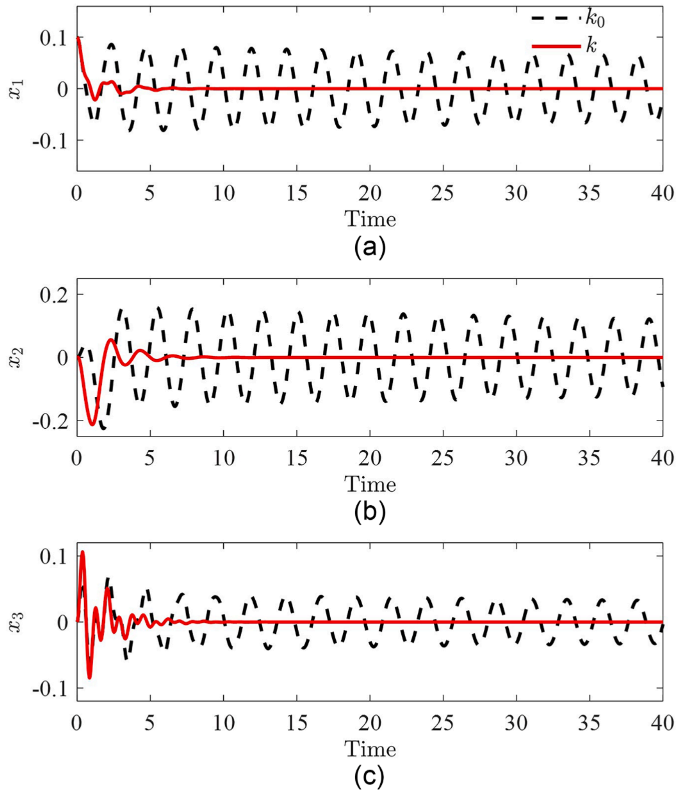

Fig. 8. Free-evolution of the closed-loop system in example 3: with k_0 (black dashed line) and with k (red line), coordinate displacements: x_1 (a), x_2 (b), x_3 (c).

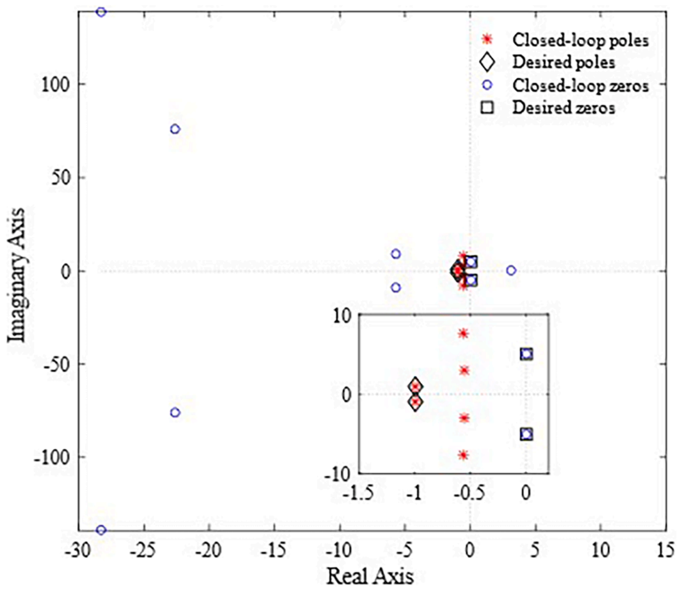

Fig. 9. Pole-zero map for the closed-loop receptance h_{21} with k in example 3.

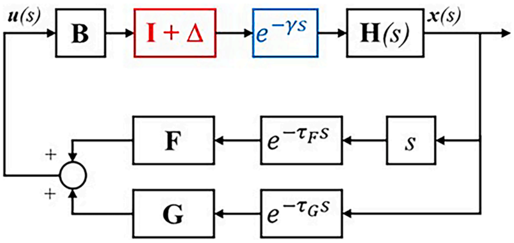

Fig. 10. Block scheme of the state feedback controlled system with gain (red) and/or delay (blue) perturbations.

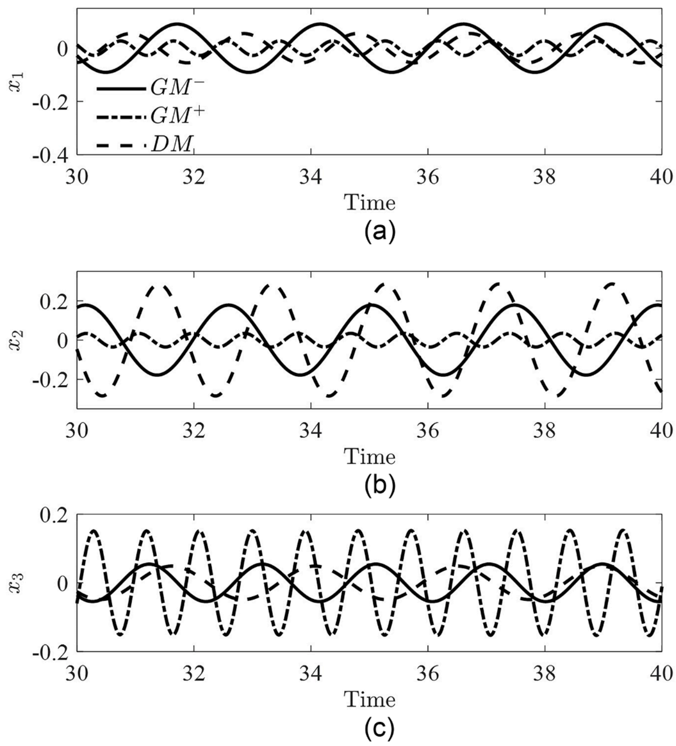

Fig. 11. Steady-state responses for the closed-loop system in example 4 with the margins computed from the eigenloci and imposed in closed-loop, coordinate displacements: x_1 (a), x_2 (b), x_3 (c).

5.4.2. *Example 6: state-derivative feedback*

The same assignment requirements as well as the same multi-step solution procedure as in Example 5 is here applied through state-derivative feedback. Fig. 14 displays the eigenloci after each step. The final control gains are: $\mathbf{D} = \begin{bmatrix} 1.3153 & -1.5683 \\ -4.5759 & 0.9572 \end{bmatrix}$, $\mathbf{F} = \begin{bmatrix} 1.6328 & -1.0380 \\ 3.7692 & -4.4636 \end{bmatrix}$. Once again, the assignment of the antiresonance is confirmed by: $\overline{h}_{22}(\pm \mathrm{i}) = (-0.1 \mp 1.1\mathrm{i})e - 16$.

For the sake of comparison, since the two designs have the same vibration suppression goal, the steady-state response of coordinate x_2 of both closed-loop systems to a harmonic disturbance with an excitation frequency equal to the chosen antiresonance frequency (e. g. $d(t) = 0.1\sin t$) applied to the same coordinate is displayed in Fig. 15. Both the designs suppress the disturbance for the response coordinate x_2 as required. The longer time taken by the state-derivative design is explained through the dominant pole $p_{\mathrm{dom}} = -0.0247 \pm 0.7861\mathrm{i}$ which is closer to the imaginary axis than that of the state-feedback design $p_{\mathrm{dom}} = -0.0838 \pm 1.2180\mathrm{i}$.

5.5. *Some notes on the computational effort*

The quantification of the computational effort for the robustification and stabilization stage is not trivial to be estimated due to stochastic nature of the GA. First, the choice of the modal vectors which in turn determines the coefficient vectors $\boldsymbol{\alpha}_{\mathbf{z}}$ and $\boldsymbol{\beta}_{\mathbf{p}}$ has a great influence on the initial solution and then in the search of a solution in the single-step case. However, for the sake of comparison in similar conditions, the computational times were estimated in Examples 5 and 6 (respectively Sections 5.4.1 and 5.4.2) and also for the

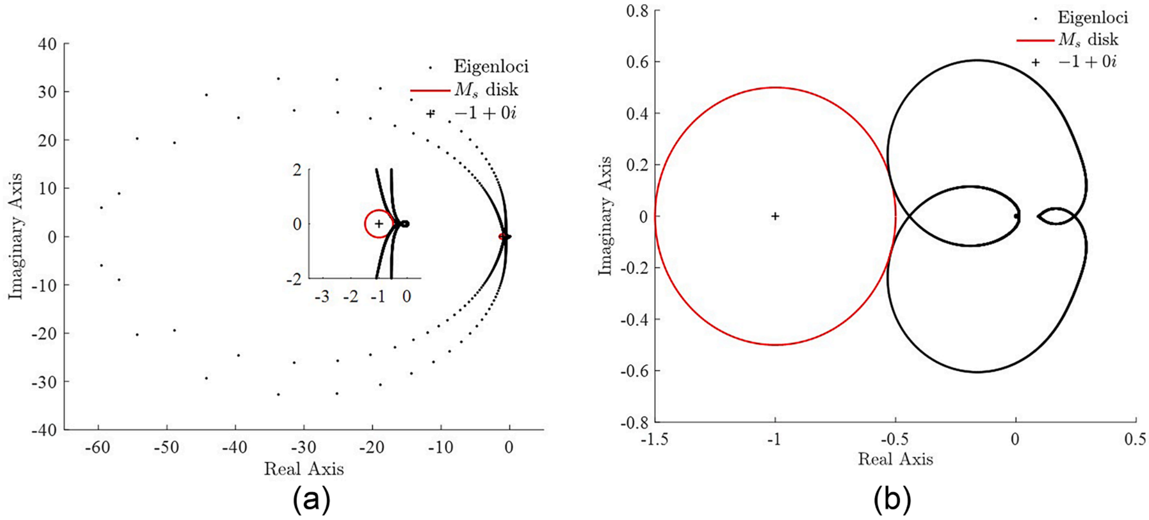

Fig. 12. The eigenloci of the system in example 5: (a) Step 1; (b) Step 2.

Table 9
Example 5: dominant poles under failure of actuator 2.

	Dominant eigenvalues	
	Multi-step	Single-step
Without failure	$-0.0838 \pm 1.2180i$	$-0.0823 \pm 0.8985i$
With a failure in the last actuator	$-0.1610 \pm 1.1442i$	$0.2251 \pm 1.0387i$

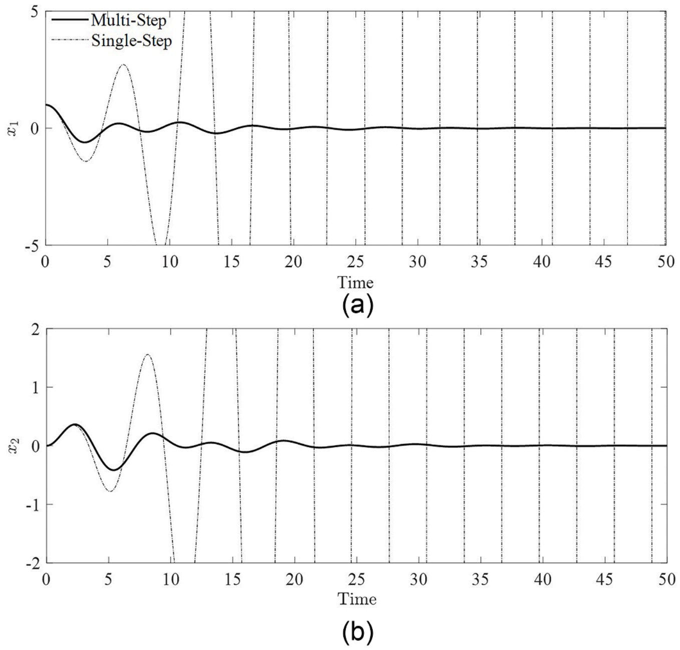

Fig. 13. Free-evolution of the closed-loop systems in example 5 under failure of the actuator $k = 2$, coordinate displacements: x_1 (a), x_2 (b).

single-step approach. An additional test has been performed applying the GA search only in the last step for the multi-step approach (multi-step non-fault tolerant approach). Table 10 compares the CPU times required to compute the final control gains with the proposed methods. The tests have been performed on an i5–8250 U CPU with 1.60 GHz and an 8.00 Gb RAM. Since the controller design is entirely performed offline, all these computational times can be considered satisfactory.

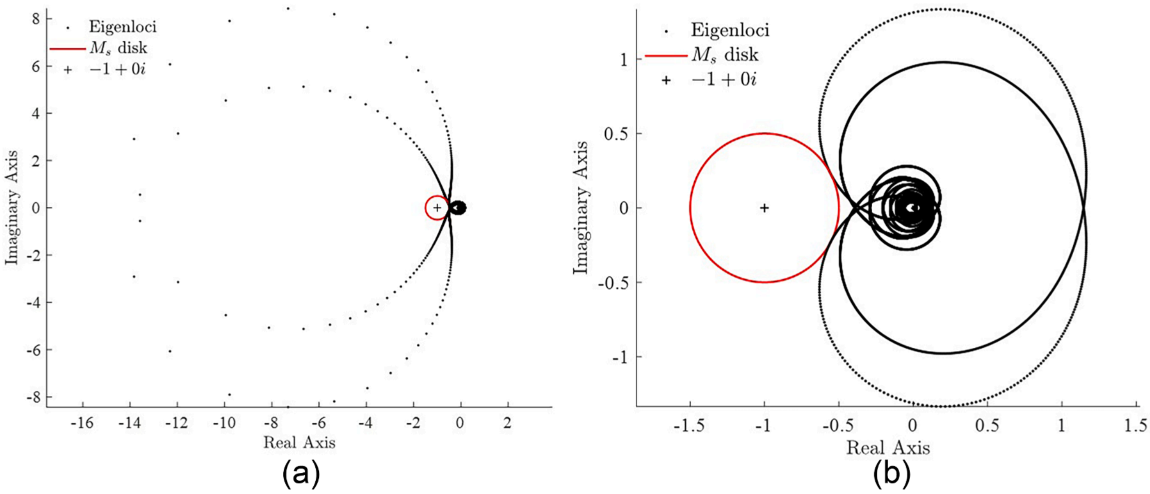

Fig. 14. The eigenloci of the system in example 6: (a) Step 1; (b) Step 2.

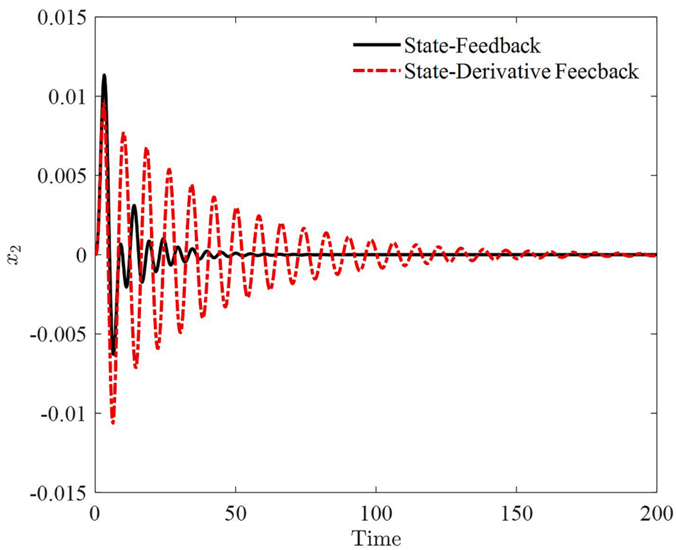

Fig. 15. Comparison of the state and state-derivative closed-loop systems in example 6: response of the output coordinate x_2 under harmonic disturbance applied to the same coordinate.

Table 10
Computational times for test-case 3.

Method	CPU Time [s]
Multi-step, state feedback, GA after each step	134
Single-step, state feedback	103
Multi-step, state-derivative feedback, GA after each step	105
Single-step, state-derivative feedback	54
Multi-step, state feedback, GA after the last step	35

5.6. Test-case 4: single-step state feedback control

In this Section the single-step method is applied to the numerical model of the experimental setup proposed in [44] exploiting state feedback control. The same parameters are adopted, i.e., $m_a = 0.52$ kg, $m_0 = 1.1750$ kg, $m_1 = 0.5050$ kg, $m_2 = 0.7290$ kg, $k_a = 407$ Nm^{-1}, $k_0 = 1001$ Nm^{-1}, $k_1 = 749$ Nm^{-1}, $k_2 = 711$ Nm^{-1}, $k_3 = 950$ Nm^{-1}, $k_4 = 377$ Nm^{-1}, $c_a = 1.8$ Nsm^{-1}, $c_0 = 4.35$ Nsm^{-1}, $c_1 = 0.85$ Nsm^{-1}, $c_2 = 1.85$ Nsm^{-1}, $c_3 = 4.95$ Nsm^{-1}, $c_4 = 0$ Nsm^{-1}. The system matrices are the following:

$$\mathbf{M} = \mathrm{diag}(m_0, m_1, m_2, m_a), \quad \mathbf{C} = \begin{bmatrix} c_0 + c_1 + c_a + c_4 & -c_1 & -c_4 & -c_a \\ -c_1 & c_1 + c_2 & -c_2 & 0 \\ -c_4 & -c_2 & c_2 + c_3 + c_4 & 0 \\ -c_a & 0 & 0 & c_a \end{bmatrix},$$
$$\mathbf{K} = \begin{bmatrix} k_0 + k_1 + k_a + k_4 & -k_1 & -k_4 & -k_a \\ -k_1 & k_1 + k_2 & -k_2 & 0 \\ -k_4 & -k_2 & k_2 + k_3 + k_4 & 0 \\ -k_a & 0 & 0 & k_a \end{bmatrix}, \quad \mathbf{B} = \begin{bmatrix} -1 & 1 \\ 0 & 0 \\ 0 & 0 \\ 1 & 0 \end{bmatrix} \tag{68}$$

The time delays assumed for both the position and velocity feedback are equal to 0.1 s. An undamped antiresonance is assigned at 5 Hz, for the cross-receptance h_{23}, i.e., the one between the disturbance acting on mass m_2 and the displacement of mass m_1. Then, the required complex conjugate pair of zeros is $\Sigma_z = \{\pm 2\pi 5\mathrm{i}\}$ and robustness is specified in the genetic algorithm by imposing $M_s = 1.667$. The proposed method is capable of assigning the required zeros as shown in Fig. 16. Besides that, robustness is witnessed by the eigenloci reported in Fig. 17. The capability of vibration suppression is assessed through the numerical simulations performed in presence of a disturbance at the same frequency of the assigned pair of zeros, the results are illustrated in Fig. 18.

6. Conclusion

This paper proposes a two stage method to perform the pole-zero assignment in multi-input vibrating systems affected by time delays in the measured signals or in the actuation forces. The method places the desired eigenvalues to perform vibration suppression and simultaneously ensures the robust stability of the closed-loop system through one *a priori* condition. The proposed technique exploits the measured receptances, i.e., it does not require the system matrices and can rely only on experimental measurements if the model of the system is not available. Additionally, both state and state-derivative feedback controllers can be designed through this approach.

The method consists in two stages: the first, assignment stage and the second, robustification stage. In the first stage: two receptance-based techniques are proposed for the zero, and pole-zero, assignment in systems with time delay. One technique relies on a single-step procedure while the other exploits a multi-step approach. The assignment stage relies on the solution of a linear system whose formulation depends on the pole-zero assignment specifications, hence the computational effort required is negligible. Then, the null space of the linear system solved is further exploited in the second stage to additionally fulfill the specification related to both

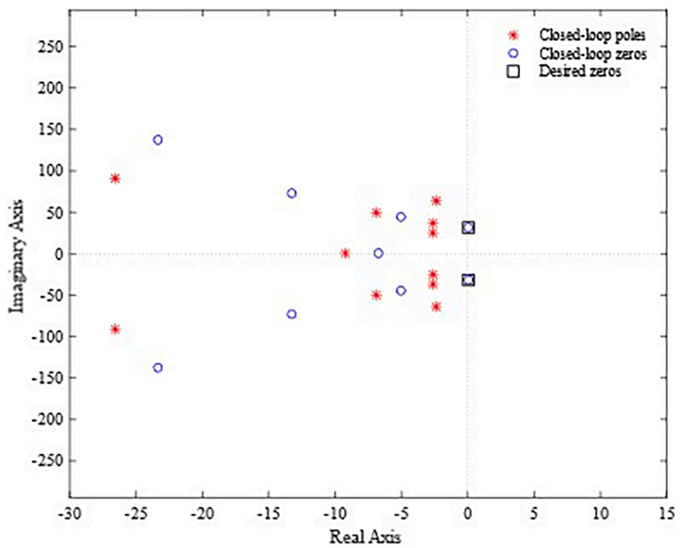

Fig. 16. Pole-zero map for the closed-loop receptance h_{23} in test-case 4.

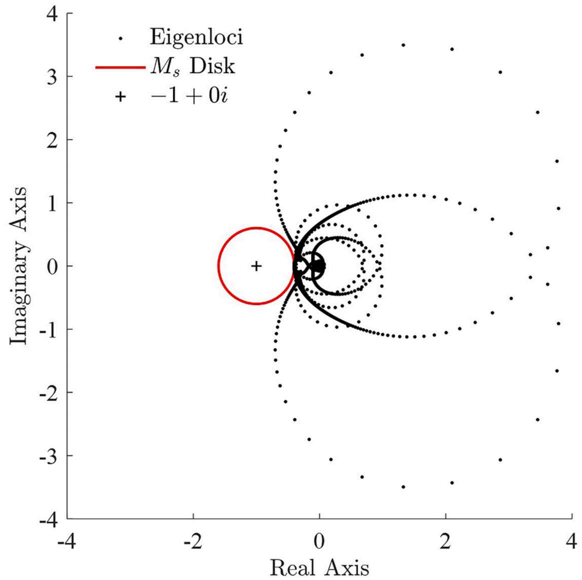

Fig. 17. The eigenloci of the closed-loop system in test-case 4.

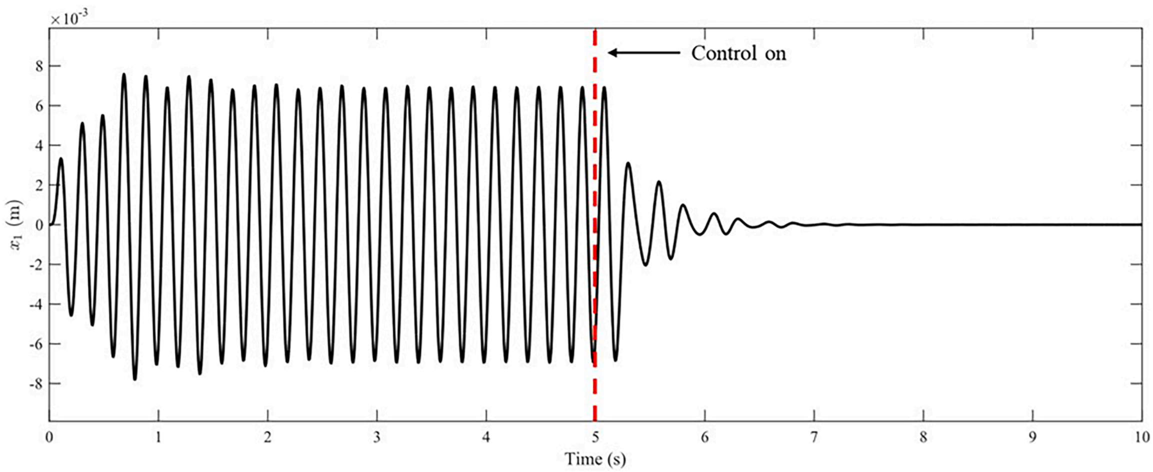

Fig. 18. Open loop and closed-loop system in test-case 4: displacements of m_1 with harmonic disturbance applied to m_2.

stability and robustness. In this light, a formulation based on the concept of eigenloci is carried out to ensure that the closed loop is robustly stable while not changing the placement of the zeros and/or poles obtained in the first stage. To cope with this task, a disk of a prescribed radius provides the measure of the distance of the eigenloci with respect to the stability critical point in the complex plane. Solving this problem and obtaining the control gains that yield the robust solution is not trivial. Hence, a genetic algorithm is developed to design the robust controller.

The single-step procedure enables to specify in the first stage, by means of the modal coefficients both the right-eigenvectors for the closed-loop adjunct system and the desired eigenvectors for the closed-loop system. On the other hand, the multi-step approach does not require to specify the closed-loop system eigenvectors but it can be exploited to provide a fault tolerant control design in the case of actuators that can fail if the Genetic Algorithm is applied for each step of the controller tuning procedure in the second stage.

The effectiveness of the proposed methods is assessed through their application on four meaningful test-cases taken from the literature and the advantages of the proposed techniques are clearly evidenced.

The main contributions with respect to the existing literature are the following:

- Two receptance-based methods for the zero assignment in multi-input vibrating systems with time-delay are proposed;
- The pole-zero placement problem is solved;

- The theory of the eigenloci is exploited to formulate a receptance-based design ensuring the a-priori stability and robustness of the closed-loop system;
- A genetic algorithm has been developed to solve the controller design problem, by also exploiting the proposed controller parameterization that reduces the number of design variables and hence boosts convergence.

CRediT authorship contribution statement

José Mário Araújo: Writing – review & editing, Writing – original draft, Visualization, Validation, Software, Methodology, Investigation, Formal analysis, Data curation, Conceptualization. **Nelson J.B. Dantas:** Visualization, Validation, Software, Methodology, Investigation, Formal analysis, Data curation, Conceptualization. **Carlos E.T. Dórea:** Supervision, Investigation, Funding acquisition, Formal analysis, Conceptualization. **Dario Richiedei:** Writing – review & editing, Writing – original draft, Supervision, Project administration, Methodology, Investigation, Funding acquisition, Formal analysis, Conceptualization. **Iacopo Tamellin:** Writing – review & editing, Writing – original draft, Visualization, Validation, Supervision, Software, Methodology, Investigation, Formal analysis, Data curation, Project administration.

Declaration of competing interest

The authors declare that they have no known competing financial interests or personal relationships that could have appeared to influence the work reported in this paper.

Funding

This research was supported by the Conselho Nacional de Desenvolvimento Científico e Tecnológico - CNPq [grant numbers 311478/2022–0, 306178/2023–0].

Appendix A. Proof of the multi-step pole-zero assignment

Let us consider the k-th stage of the multi-step method. The closed-loop receptance matrix at the k-th stage is $\overline{\mathbf{H}}_k(s) = \left(s^2\mathbf{M} + s\left(\mathbf{C}_{k-1} - \mathbf{b}_k\mathbf{f}_k^T\mathrm{e}^{-s\tau_F}\right) + \left(\mathbf{K}_{k-1} - \mathbf{b}_k\mathbf{g}_k^T\mathrm{e}^{-s\tau_G}\right)\right)^{-1}$. This equation is similar to that of the single-input control proposed in [5]. The differences are two: first, two time delays τ_F and τ_G are considered. Second, the stiffness and damping matrices ($\mathbf{K}_{k-1}$ and $\mathbf{C}_{k-1}$) are here modified through the displacement and velocity gains computed in the previous k-1 stages as described in Section 3.1.2.

In the state feedback scenario, at the k-th step of the method, the control gains, f_k and g_k that place the prescribed zeros and/or poles have to be computed.

Let us consider the zero placement. For the prescribed zeros $\overline{z}_{i,k}$, $i = 1, \dots, n_z$ of $\overline{h}_{pq,k}$ the numerator in Eq. (27) vanishes, i.e.,:

$$\mathbf{e}_p^T\left[\left(1 - \left(\overline{z}_{i,k}\mathbf{f}_k\mathrm{e}^{-\overline{z}_{i,k}\tau_F} + \mathbf{g}_k\mathrm{e}^{-\overline{z}_{i,k}\tau_G}\right)^T\overline{\mathbf{H}}_{k-1}\left(\overline{z}_{i,k}\right)\mathbf{b}_k\right)\overline{\mathbf{H}}_{k-1}\left(\overline{z}_{i,k}\right) + \overline{\mathbf{H}}_{k-1}\left(\overline{z}_{i,k}\right)\mathbf{b}_k\left(\overline{z}_{i,k}\mathbf{f}_k\mathrm{e}^{-\overline{z}_{i,k}\tau_F} + \mathbf{g}_k\mathrm{e}^{-\overline{z}_{i,k}\tau_G}\right)^T\overline{\mathbf{H}}_{k-1}\left(\overline{z}_{i,k}\right)\right]\mathbf{e}_q = 0 \tag{A.1}$$

The scalar $\overline{h}_{pq,k-1}\left(\overline{z}_{i,k}\right) = \mathbf{e}_p^T\overline{\mathbf{H}}_{k-1}\left(\overline{z}_{i,k}\right)\mathbf{e}_q$ is defined, then the substitution of $\mathbf{t}_{i,k} = \overline{h}_{pq,k-1}\left(\overline{z}_{i,k}\right)\overline{\mathbf{H}}_{k-1}\left(\overline{z}_{i,k}\right)\mathbf{b}_k - \left[\mathbf{e}_p^T\overline{\mathbf{H}}_{k-1}\left(\overline{z}_{i,k}\right)\mathbf{b}_k\right]\overline{\mathbf{H}}_{k-1}\left(\overline{z}_{i,k}\right)\mathbf{e}_q$ in Eq. (A.1) provides the compact form:

$$\left(\overline{z}_{i,k}\mathbf{f}_k\mathrm{e}^{-\overline{z}_{i,k}\tau_F} + \mathbf{g}_k\mathrm{e}^{-\overline{z}_{i,k}\tau_G}\right)^T\mathbf{t}_{i,k} = \overline{h}_{pq,k-1}\left(\overline{z}_{i,k}\right), \quad i = 1, \dots, n_z \tag{A.2}$$

The zero assignment is solved by finding the control gains f_k and g_k that satisfy Eq. (A.2) for $i = 1, \dots, n_z$. Hence, the linear system in Eq. (28) is obtained.

Let us now consider the pole assignment problem. The prescribed poles $\overline{p}_{i,k}$, $i = 1, \dots, n_p$ are assigned through the control gains f_k and g_k that make the denominator in Eq. (27) null:

$$1 - \left(\overline{p}_{i,k}\mathbf{f}_k\mathrm{e}^{-\overline{p}_{i,k}\tau_F} + \mathbf{g}_k\mathrm{e}^{-\overline{p}_{i,k}\tau_G}\right)^T\overline{\mathbf{H}}_{k-1}\left(\overline{p}_{i,k}\right)\mathbf{b}_k = 0 \tag{A.3}$$

A more compact form is obtained by defining $\mathbf{r}_{i,k} = \overline{\mathbf{H}}_{k-1}\left(\overline{p}_{i,k}\right)\mathbf{b}_k$ in Eq. (A.3):

$$\left(\overline{p}_{i,k}\mathbf{f}_k\mathrm{e}^{-\overline{p}_{i,k}\tau_F} + \mathbf{g}_k\mathrm{e}^{-\overline{p}_{i,k}\tau_G}\right)^T\mathbf{r}_{i,k} = 1 \tag{A.4}$$

The control gains f_k and g_k are obtained by solving Eq. (A.4) for the n_p prescribed poles that solve, i.e., the linear system in Eq. (42).

The demonstration in the scenario of state-derivative feedback is straightforward since it follows the same steps provided in the previous equations by just redefining Eq. (27) into its counterpart for state-derivative control, i.e.,:

$$\overline{h}_{pq,k}(s) = \frac{\mathbf{e}_p^T\left[\left(1 - \left(s^2\mathbf{d}_k\mathrm{e}^{-s\tau_D} + s\mathbf{f}_k\mathrm{e}^{-s\tau_F}\right)^T\overline{\mathbf{H}}_{k-1}(s)\mathbf{b}_k\right)\overline{\mathbf{H}}_{k-1}(s) + \overline{\mathbf{H}}_{k-1}(s)\mathbf{b}_k\left(s^2\mathbf{d}_k\mathrm{e}^{-s\tau_D} + s\mathbf{f}_k\mathrm{e}^{-s\tau_F}\right)^T\overline{\mathbf{H}}_{k-1}(s)\right]\mathbf{e}_q}{1 - \left(s^2\mathbf{d}_k\mathrm{e}^{-s\tau_D} + s\mathbf{f}_k\mathrm{e}^{-s\tau_F}\right)^T\overline{\mathbf{H}}_{k-1}(s)\mathbf{b}_k} \tag{A.5}$$

Data availability

Data will be made available on request.

References

[1] Y.M. Ram, J.E. Mottershead, Receptance method in active vibration control, AIAA J. 45 (2007) 562–567, https://doi.org/10.2514/1.24349.
[2] Y.M. Ram, J.E. Mottershead, Multiple-input active vibration control by partial pole placement using the method of receptances, Mech. Syst. Signal. Process. 40 (2013) 727–735, https://doi.org/10.1016/j.ymssp.2013.06.008.
[3] L. Mirkin, Z.J. Palmor, Control issues in systems with loop delays, in: Handbook of networked and embedded control systems, Birkhäuser Boston, Boston, MA, 2005, pp. 627–648, https://doi.org/10.1007/0-8176-4404-0_27.
[4] Y.M. Ram, A. Singh, J.E. Mottershead, State feedback control with time delay, Mech. Syst. Signal. Process. 23 (2009) 1940–1945, https://doi.org/10.1016/j.ymssp.2008.04.012.
[5] Y.M. Ram, J.E. Mottershead, M.G. Tehrani, Partial pole placement with time delay in structures using the receptance and the system matrices, Linear. Algebra Appl. 434 (2011) 1689–1696, https://doi.org/10.1016/j.laa.2010.07.014.
[6] J. Xiang, C. Zhen, D. Li, Partial pole assignment with time delay by the receptance method using multi-input control from measurement output feedback, Mech. Syst. Signal. Process. (2016), https://doi.org/10.1016/j.ymssp.2015.06.003.
[7] L. Zhang, Multi-input partial eigenvalue assignment for high order control systems with time delay, Mech. Syst. Signal. Process. 72–73 (2016) 376–382, https://doi.org/10.1016/j.ymssp.2015.09.033.
[8] X.T. Wang, L. Zhang, Partial eigenvalue assignment with time delay in high order system using the receptance, Linear. Algebra Appl. 523 (2017) 335–345, https://doi.org/10.1016/j.laa.2017.02.034.
[9] K. Engelborghs, T. Luzyanina, D. Roose, Numerical bifurcation analysis of delay differential equations using DDE-BIFTOOL, ACM Transact. Math. Software 28 (2002) 1–21, https://doi.org/10.1145/513001.513002.
[10] J.-F. Zhang, H. Ouyang, K.-W. Zhang, H.-M. Liu, Stability test and dominant eigenvalues computation for second-order linear systems with multiple time-delays using receptance method, Mech. Syst. Signal. Process. 137 (2020) 106180, https://doi.org/10.1016/j.ymssp.2019.05.064.
[11] Z.-H. Lv, J.-F. Zhang, H. Ouyang, Receptance-based computation of stability crossing curves for single-input-multiple-output second-order linear systems with two time-delays, Internat. J. Struct. Stab. Dyn. 22 (2022), https://doi.org/10.1142/S021945542250002X.
[12] F.O. Souza, Critical frequencies of controlled second-order linear systems with delayed feedback, Mech. Syst. Signal. Process. 166 (2022) 108384, https://doi.org/10.1016/j.ymssp.2021.108384.
[13] N. Olgac, R. Sipahi, An exact method for the stability analysis of time-delayed linear time-invariant (LTI) systems, IEEe Trans. Automat. Contr. 47 (2002) 793–797, https://doi.org/10.1109/TAC.2002.1000275.
[14] R. Belotti, D. Richiedei, Pole assignment in vibrating systems with time delay: an approach embedding an a-priori stability condition based on Linear Matrix Inequality, Mech. Syst. Signal. Process. 137 (2020) 106396, https://doi.org/10.1016/j.ymssp.2019.106396.
[15] J.M. Araújo, Discussion on 'State feedback control with time delay, Mech. Syst. Signal. Process. (2018), https://doi.org/10.1016/j.ymssp.2017.05.004.
[16] N.J.B. Dantas, C.E.T. Dórea, J.M. Araújo, Design of rank-one modification feedback controllers for second-order systems with time delay using frequency response methods, Mech. Syst. Signal. Process. 137 (2020) 106404, https://doi.org/10.1016/j.ymssp.2019.106404.
[17] N.J.B. Dantas, C.E.T. Dorea, J.M. Araujo, Partial pole assignment using rank-one control and receptance in second-order systems with time delay, Meccanica 56 (2021), https://doi.org/10.1007/s11012-020-01289-w.
[18] J.M. Araújo, J. Bettega, N.J.B. Dantas, C.E.T. Dórea, D. Richiedei, I. Tamellin, Vibration control of a two-link flexible robot arm with time delay through the robust receptance method, Appl. Sci. 11 (2021) 9907, https://doi.org/10.3390/app11219907.
[19] D. Richiedei, I. Tamellin, A. Trevisani, Pole-zero assignment by the receptance method: multi-input active vibration control, Mech. Syst. Signal. Process. 172 (2022) 108976, https://doi.org/10.1016/j.ymssp.2022.108976.
[20] C. Desoer, Yung-Terng Wang, On the generalized nyquist stability criterion, IEEe Trans. Automat. Contr. 25 (1980) 187–196, https://doi.org/10.1109/TAC.1980.1102280.
[21] S.H. Tsai, H. Ouyang, J.Y. Chang, Inverse structural modifications of a geared rotor-bearing system for frequency assignment using measured receptances, Mech. Syst. Signal. Process. 110 (2018) 59–72, https://doi.org/10.1016/j.ymssp.2018.03.008.
[22] D. Richiedei, I. Tamellin, A. Trevisani, Beyond the tuned mass damper: a comparative study of passive approaches to vibration absorption through antiresonance assignment, Arch. Computat. Methods Eng. (2021), https://doi.org/10.1007/s11831-021-09583-w.
[23] B.P. Wang, Antiresonance and its sensitivity analysis in structural systems, in: Collection of technical papers - AIAA/ASME/ASCE/AHS/ASC structures, structural dynamics and materials conference, 1998, https://doi.org/10.2514/6.1998-1751.
[24] J.E. Mottershead, M.G. Tehrani, S. James, P. Court, Active vibration control experiments on an AgustaWestland W30 helicopter airframe, Proc. Inst. Mech. Eng. C. J. Mech. Eng. Sci. 226 (2012) 1504–1516, https://doi.org/10.1177/0954406211423609.
[25] M. Ghandchi Tehrani, J.E. Mottershead, A.T. Shenton, Y.M. Ram, Robust pole placement in structures by the method of receptances, Mech. Syst. Signal. Process. (2011), https://doi.org/10.1016/j.ymssp.2010.04.005.
[26] L.J. Adamson, S. Fichera, J.E. Mottershead, Receptance-based robust eigenstructure assignment, Mech. Syst. Signal. Process. 120 (2020) 106697, https://doi.org/10.1016/j.ymssp.2020.106697.
[27] B. Mokrani, A. Batou, S. Fichera, L. Adamson, D. Alaluf, J.E. Mottershead, The minimum norm multi-input multi-output receptance method for partial pole placement, Mech. Syst. Signal. Process. (2019), https://doi.org/10.1016/j.ymssp.2019.03.003.
[28] R. Ariyatanapol, Y.P. Xiong, H. Ouyang, Partial pole assignment with time delays for asymmetric systems, Acta Mech. (2018) 229, https://doi.org/10.1007/s00707-018-2118-2.
[29] A. Ben-Israel, T.N.E. Greville, Generalized inverses, theory and applications, 2nd ed., Springer-Verlag, New York, 2003 https://doi.org/10.1007/b97366.
[30] Z. Wang, J. Zhang, L. Yang, Weighted pseudo-inverse based control allocation of heterogeneous redundant operating mechanisms for distributed propulsion configuration, Energy Procedia 158 (2019) 1718–1723, https://doi.org/10.1016/j.egypro.2019.01.400.
[31] D. Richiedei, I. Tamellin, Active control of linear vibrating systems for antiresonance assignment with regional pole placement, J. Sound. Vib. 494 (2021) 115858, https://doi.org/10.1016/j.jsv.2020.115858.
[32] R. Belotti, D. Richiedei, I. Tamellin, Pole assignment for active vibration control of linear vibrating systems through linear matrix inequalities, Appl. Sci. 10 (2020) 5494, https://doi.org/10.3390/app10165494.
[33] A.G.J. MacFarlane, I. Postelthwaite, The generalized Nyquist stability criterion and multivariable root loci, Int. J. Control 25 (1977) 81–127, https://doi.org/10.1080/00207177708922217.
[34] C. Desoer, Yung-Terng Wang, On the generalized nyquist stability criterion, IEEe Trans. Automat. Contr. 25 (1980) 187–196, https://doi.org/10.1109/TAC.1980.1102280.
[35] H.V. Henderson, S.R. Searle, On deriving the inverse of a sum of matrices, SIAM Rev. 23 (1981) 53–60, https://doi.org/10.1137/1023004.
[36] P. Seiler, A. Packard, P. Gahinet, An introduction to disk margins [Lecture Notes], IEEe Control Syst. 40 (2020) 78–95, https://doi.org/10.1109/MCS.2020.3005277.
[37] S. Skogestad, I. Postlethwaite, Multivariable feedback control: analysis and design, 2nd ed., JOHN WILEY & SONS, New York, 2005.
[38] M. Sami Fadali, A. Visioli, Digital Control Engineering, 3rd ed., Elsevier, 2020 https://doi.org/10.1016/C2017-0-01563-X.
[39] L. Zhang, T. Zhang, H. Ouyang, T. Li, Receptance-based antiresonant frequency assignment of an uncertain dynamic system using interval multiobjective optimization method, J. Sound. Vib. 529 (2022) 116944, https://doi.org/10.1016/j.jsv.2022.116944.

[40] T.H.S. Abdelaziz, Robust pole assignment using velocity-acceleration feedback for second-order dynamical systems with singular mass matrix, ISA Trans. (2015), https://doi.org/10.1016/j.isatra.2014.11.015.
[41] F. Tisseur, N.J. Higham, Structured pseudospectra for polynomial eigenvalue problems, with applications, SIAM J. Matrix Analy. Applic. 23 (2001) 187–208, https://doi.org/10.1137/S0895479800371451.
[42] R.H. Middleton, D.E. Miller, On the achievable delay margin using LTI control for unstable plants, IEEe Trans. Automat. Contr. 52 (2007) 1194–1207, https://doi.org/10.1109/TAC.2007.900824.
[43] A. Shapiro, Stability of second-order asymmetric linear mechanical systems with application to robot grasping, J. Appl. Mech. 72 (2005) 966–968, https://doi.org/10.1115/1.2042484.
[44] A. Saldanha, W. Michiels, M. Kuře, J. Bušek, T. Vyhlídal, Stability optimization of time-delay systems with zero-location constraints applied to non-collocated vibration suppression, Mech. Syst. Signal. Process. 208 (2024) 110886, https://doi.org/10.1016/j.ymssp.2023.110886.